RUSSIAN MARITIME REGISTER OF SHIPPING

CIRCULAR LETTER	No. 314-01-1491c	dated 28.12.2020

Re:

amendments to the Rules for the Classification and Construction of Sea-Going Ships considering experience in application of the Rules

Item(s) of supervision:

ships under construction

Entry-into-force date: **01.02.2021**	~~Valid till:~~	~~Validity period extended till:~~

~~Cancels / amends / adds Circular Letter No.~~	~~dated~~

Number of pages:	1 + 41

Appendices:

Appendix 1: information on amendments introduced by the Circular Letter

Appendix 2: text of amendments to Part XVI "Structure and Strength of Fiber-Reinforced Plastic Ships"

Director General	Konstantin G. Palnikov

Text of CL:

We hereby inform that the Rules for the Classification and Construction of Sea-Going Ships shall be amended after re-publication in 2021 as specified in the Appendices to the Circular Letter.

It is necessary to do the following:

1. Bring the content of the Circular Letter to the notice of the RS surveyors, interested organizations and persons in the area of the RS Branch Offices' activity.

2. Apply the provisions of the Circular Letter during review and approval of the technical documentation on ships contracted for construction or conversion on or after 01.02.2021, in the absence of a contract, the keels of which are laid or which are at a similar stage of construction on or after 01.02.2021, as well as during review and approval of the technical documentation on ships, the delivery of which is on or after 01.02.2021.

List of the amended and/or introduced paras/chapters/sections:

Section 2: paras 2.2.1, 2.2.4, Tables 2.1 — 2.5;

Section 3: Figures 3.1 — 3.31, para 3.2.6.2.2, Figure 3.32, para 3.2.6.2.4, Figure 3.33, paras 3.2.6.2.5, 3.2.6.3.2, Figure 3.34, para 3.2.6.3.4, Figures 3.35 — 3.39, para 3.2.6.3.9, Figures 3.40 — 3.54;

Section 4: Figure 4;

Section 5: Tables 5.1 and 5.2, Figures 5.1 and 5.2;

Appendix 1: Figure 1, para 1.1, Figure 2, Table 1, paras 2.1 and 2.2, Section 3, paras 4.1 — 4.3, Figures 4 — 6, Table 4, paras 5.1 — 5.3, Tables 5 and 6, Figures 7 and 8, Section 6, Table 7, Section 7, Table 8, paras 8.1 and 8.2, Figures 9 — 24, paras 8.3 and 8.4, Figures 25 — 29, paras 9.1 — 9.3, Figures 30 — 35

Person in charge:	Sergey M. Kordonets	314	+7 812 3128572

"Thesis" System No.	20-217481

**Information on amendments introduced by the Circular Letter
(for inclusion in the Revision History to the RS Publication)**

Nos.	Amended paras/chapters/sections	Information on amendments	Number and date of the Circular Letter	Entry-into-force date
1	Paras 2.2.1, 2.2.4	Requirement for execution of type approval of FRPs has been specified	314-01-1491c of 28.12.2020	01.02.2021
2	Chapter 2.3	Consecutive numbering of Tables 2.1 — 2.5 has been replaced by numbering which correlates with the numbers of paras	314-01-1491c of 28.12.2020	01.02.2021
3	Chapter 3.1	Consecutive numbering of Figures 3.1 and 3.2 has been replaced by numbering which correlates with the numbers of paras	314-01-1491c of 28.12.2020	01.02.2021
4	Chapter 3.2	Consecutive numbering of Figures 3.3 — 3.49 and Table 3.1 has been replaced by numbering which correlates with the numbers of paras	314-01-1491c of 28.12.2020	01.02.2021
5	Figure 3.2.1.1.8 (former Figure 3.8)	Symbols S_{01} and S_{02} have been replaced by S_0 and S_1	314-01-1491c of 28.12.2020	01.02.2021
6	Figure 3.2.2.2.9 (former Figure 3.13)	Symbol S_s has been replaced by S_s^2	314-01-1491c of 28.12.2020	01.02.2021
7	Figure 3.2.6.2.2 (former Figure 3.31)	Repeated symbols $b_c{}^1$, $t_c{}^1$ have been replaced by b_c^n, b_c^i, $b_c{}^1$ and $t_c{}^1$	314-01-1491c of 28.12.2020	01.02.2021
8	Para 3.2.6.2.2	Parameters of straps for joints without edge preparation have been specified	314-01-1491c of 28.12.2020	01.02.2021
9	Figure 3.2.6.2.4 (former Figure 3.32)	Symbol t_{over} has been repositioned. Setup has been modified in area of b_m (symbols b_r, b_n have been introduced)	314-01-1491c of 28.12.2020	01.02.2021
10	Para 3.2.6.2.4	Butt joint parameters of sandwich members have been specified	314-01-1491c of 28.12.2020	01.02.2021
11	Figure 3.2.6.2.5 (former Figure 3.33)	Symbols have been specified	314-01-1491c of 28.12.2020	01.02.2021
12	Para 3.2.6.2.5	Symbol b_c has been replaced by b_s	314-01-1491c of 28.12.2020	01.02.2021
13	Para 3.2.6.3.2	Dimension "mm" has been added to parameter s	314-01-1491c of 28.12.2020	01.02.2021
14	Figure 3.2.6.3.2 (former Figure 3.34)	Symbol R_{angl} has been repositioned	314-01-1491c of 28.12.2020	01.02.2021

Nos.	Amended paras/chapters/sections	Information on amendments	Number and date of the Circular Letter	Entry-into-force date
15	Para 3.2.6.3.4	Requirements for foam plastic in cores of the bulkhead in the area of joint with single-skin hull have been specified. Parameters for determination of thickened area scantlings have been specified	314-01-1491c of 28.12.2020	01.02.2021
16	Figure 3.2.6.3.7 (former Figure 3.37)	Symbol t_{angl}^{out} has been replaced by b_{angl}^{out}, symbol $1S$ has been replaced by 15, symbol t_{angl}^{in} has been replaced by t_{angl}^{out}	314-01-1491c of 28.12.2020	01.02.2021
17	Figure 3.2.6.3.8-1 (former Figure 3.38)	Symbol $1S$ has been replaced by 15, symbol t_{angl}^{in} has been replaced by t_{angl}^{out}	314-01-1491c of 28.12.2020	01.02.2021
18	Para 3.2.6.3.9	Basic parameters of joints of the inner deck (platform) with a single-skin and sandwich side plating have been specified	314-01-1491c of 28.12.2020	01.02.2021
19	Chapter 3.3	Consecutive numbering of Figures 3.50 — 3.54 has been replaced by numbering which correlates with the numbers of paras	314-01-1491c of 28.12.2020	01.02.2021
20	Chapter 4.2	Figure 4.1 and references thereto have been renumbered 4.2.1	314-01-1491c of 28.12.2020	01.02.2021
21	Chapter 5.3	Consecutive numbering of Tables 5.1 and 5.2 and Figures 5.1 and 5.2 has been replaced by numbering which correlates with the numbers of paras	314-01-1491c of 28.12.2020	01.02.2021
22	Appendix 1, Section 1	Consecutive numbering of Table 1 and Figures 1 and 2 has been replaced by numbering which correlates with the numbers of paras	314-01-1491c of 28.12.2020	01.02.2021
23	Appendix 1, Figure 1.1 (former Figure 1)	Vertical axis Z(3) has been added	314-01-1491c of 28.12.2020	01.02.2021
24	Appendix 1, para 1.1	Formula for determination of member cross-section shear stiffness has been introduced	314-01-1491c of 28.12.2020	01.02.2021
25	Appendix 1, para 2.1	Formula for determination of shear stiffness has been deleted	314-01-1491c of 28.12.2020	01.02.2021

Nos.	Amended paras/chapters/sections	Information on amendments	Number and date of the Circular Letter	Entry-into-force date
26	Appendix 1, para 2.2	Definition of member span, has been introduced into explication to formula	314-01-1491c of 28.12.2020	01.02.2021
27	Appendix 1, Section 3	Consecutive numbering of Tables 2 and 3 has been replaced by numbering which correlates with the numbers of paras. Definitions in explication to formulae for definition of shear strain-stress behavior of single-skin plates have been specified	314-01-1491c of 28.12.2020	01.02.2021
28	Appendix 1, Section 4	Consecutive numbering of Table 4 and Figures 4 — 6 has been replaced by numbering which correlates with the numbers of paras	314-01-1491c of 28.12.2020	01.02.2021
29	Appendix 1, para 4.1	New para 4.1 has been introduced containing requirements for determination of buckling strength of freely supported single-skin plates in compression. Existing paras 4.1 and 4.2 have been renumbered 4.2 and 4.3 accordingly	314-01-1491c of 28.12.2020	01.02.2021
30	Appendix 1, paras 4.2 and 4.3	Requirements have been specified for FRPs with parallel, and parallel and diagonal reinforcement schemes	314-01-1491c of 28.12.2020	01.02.2021
31	Appendix 1, Figures 4.3-1 — 4.3-3 (former Figures 4 — 6)	Symbols G_{12}^{bl} have been replaced by G_{12} and symbols E_p^{bl} have been replaced by E_1	314-01-1491c of 28.12.2020	01.02.2021
32	Appendix 1, Table 4.3 (former Table 4)	Symbols G_{12}^{bl} have been replaced by G_{12} and symbols E_p^{bl} have been replaced by E_1	314-01-1491c of 28.12.2020	01.02.2021
33	Appendix 1, Section 5	Consecutive numbering of Tables 5 and 6 and Figures 7 and 8 has been replaced by numbering which correlates with the numbers of paras	314-01-1491c of 28.12.2020	01.02.2021
34	Appendix 1, para 5.1	New para 5.1 has been introduced containing requirements for determination of shear buckling strength of freely supported single-skin	314-01-1491c of 28.12.2020	01.02.2021

Nos.	Amended paras/chapters/sections	Information on amendments	Number and date of the Circular Letter	Entry-into-force date
		plates. Existing paras 5.1.1 and 5.1.2 have been renumbered 5.2 and 5.3 accordingly		
35	Appendix 1, paras 5.2 and 5.3	Requirements for determination of shear critical stress have been specified	314-01-1491c of 28.12.2020	01.02.2021
36	Appendix 1, Figures 5.2 — 5.3 (former Figures 7 — 8)	Symbols G_{12}^{bl} have been replaced by G_{12} and symbols E_p^{bl} have been replaced by E_1	314-01-1491c of 28.12.2020	01.02.2021
37	Appendix 1, Table 5.2 (former table 5)	Symbols G_{12}^{bl} have been replaced by G_{12} and symbols E_p^{bl} have been replaced by E_1	314-01-1491c of 28.12.2020	01.02.2021
38	Appendix 1, Section 6	Figure 6 has been introduced. Table 7 and references thereto have been renumbered 6	314-01-1491c of 28.12.2020	01.02.2021
39	Appendix 1, Table 7 (former Table 6)	Requirements for all types of load have been specified	314-01-1491c of 28.12.2020	01.02.2021
40	Appendix 1, Section 7	Formulae to determine maximum deflections, maximum normal stresses in load-bearing layers and maximum shear stresses in the core for symmetric sandwich plates with isotropic core of the FRP hull structures have been specified. Table 8 and references thereto have been renumbered 7	314-01-1491c of 28.12.2020	01.02.2021
41	Appendix 1, Table 8 (former Table 7)	Requirements have been specified for types of load "The plate is loaded with the moment uniformly distributed over the plate's width in any section", "The transverse load is uniformly distributed in the local region of the plate in any area", "The transverse load distributed according to the triangular law is applied in the local region of the plate in any area"	314-01-1491c of 28.12.2020	01.02.2021
42	Appendix 1, Section 8	Consecutive numbering of Figures 9 — 29 has been replaced by numbering which correlates with the numbers of paras. List of	314-01-1491c of 28.12.2020	01.02.2021

Nos.	Amended paras/chapters/sections	Information on amendments	Number and date of the Circular Letter	Entry-into-force date
		symbols has been introduced. Captions of figures have been specified. Requirements for the type of load "Plate edges are fixed along the supporting contour" have been transferred into new para 8.4		
43	Appendix 1, Section 9	Consecutive numbering of Figures 30 — 35 has been replaced by numbering which correlates with the numbers of paras	314-01-1491c of 28.12.2020	01.02.2021
44	Appendix 1, paras 9.1 — 9.3	Text of preamble has been transferred into new para 9.1. Existing paras 9.1 — 9.2 have been renumbered 9.2 — 9.3 accordingly	314-01-1491c of 28.12.2020	01.02.2021
45	Appendix 1, para 9.1	Conditions to be met for load-bearing layers and the core, as well as for geometric properties and elastic characteristics of plates have been specified	314-01-1491c of 28.12.2020	01.02.2021
46	Appendix 1, para 9.3 (former para 9.2)	Requirements for determination of buckling load have been specified	314-01-1491c of 28.12.2020	01.02.2021

RULES FOR THE CLASSIFICATION AND CONSTRUCTION
OF SEA-GOING SHIPS, 2020,

ND No. 2-020101-124-E

PART XVI. STRUCTURE AND STRENGTH OF FIBER-REINFORCED PLASTIC SHIPS

2 MATERIALS

1   **Para 2.2.1** is replaced by the following text:

"**2.2.1**   FRP intended for manufacture of hulls or ship structures, as well as binders for manufacture of FRPs and cores shall be approved by the Register (provided with Type Approval Certificate (CTO) and/or Register Certificate per batch) in accordance with Part I "General Regulations for Technical Supervision" of the Rules for Technical Supervision during Construction of Ships and Manufacture of Materials and Products for Ships. The Register Certificate for FRP is not required provided the requirements specified in 2.2.4.3 of this Part of the Rules are met. Application of FRP binders for boats is allowed based on the report documents of firms (manufacturers) or laboratories recognized by the Register.

Register approval for reinforcement materials applied for FRP manufacture is recommended (refer to 2.3.1.6).".

2   **Para 2.2.4** is replaced by the following text:

"**2.2.4   Technical supervision during manufacture of hull/structures using FRP.**
2.2.4.1   Prior to manufacture, the manufacturer (a shipyard) shall submit the following:

approved technical documentation in the scope specified in 1.4.2 (technical specifications on FRPs, technological instruction);

reports on fire safety test results of FRPs carried out in laboratories recognized by the Register, with a conclusion on compliance of the fire protection with the requirements of these Rules according to which the ship design is approved;

where FRPs other than those stated in this Part of the Rules are used, reports on FRP test results in accordance with the approved test program (refer to Appendix 2).
2.2.4.2   Technical supervision shall include the following:

review of documents submitted by the firm (manufacturer) in a scope specified in 2.2.3.2 to confirm its capability of manufacturing FRP products of stable quality in required volumes;

survey of the firm (manufacturer) to assess its capability of manufacturing FRP hulls/structures and quality control systems;

technical supervision during manufacture in a scope specified in 1.5.1;

technical supervision during tests of FRP specimens cut out from manufacturing allowances or witness sample (as applicable), complying with the technical documentation on the product manufactured;

technical supervision of hull defects detection and repair.

Upon results of technical supervision during construction of hull or structure using FRPs, the report documents of shipyard shall be signed by the Register surveyor in accordance with the provisions of Section 13 "Technical Supervision at the Shipyard during Construction of Ships", Part I of the Rules for Technical Supervision during Construction of Ships and Manufacture of Materials and Products for Ships, attaching Register Certificates for materials.
2.2.4.3   Where the Register Certificate for FRP is not available during technical supervision in the course of construction of hull or structure using FRPs, in addition to the requirements specified in Section 13 "Technical Supervision at the Shipyard during Construction of Ships", Part I of the Rules for Technical Supervision during Construction of Ships and Manufacture of Materials

and Products for Ships the Report on Survey (form 6.3.29) shall be drawn up to confirm that the requirements for FRP specified in this Part of the Rules are met.".

3   **Table 2.1** and references thereto are renumbered **2.3.1.3**.

4   **Table 2.2** and references thereto are renumbered **2.3.2.2**.

5   **Table 2.3** and references thereto are renumbered **2.3.3.8**.

6   **Table 2.4** and references thereto are renumbered **2.3.5.9**.

7   **Table 2.5** and references thereto are renumbered **2.3.5.11**.

3 HULL AND SUPERSTRUCTURES OF SHIPS

8   **Figure 3.1** and references thereto are renumbered **3.1.1**.

9   **Figure 3.2** and references thereto are renumbered **3.1.3**.

10   **Figure 3.3** and references thereto are renumbered **3.1.7**.

11   **Figure 3.4** and references thereto are renumbered **3.2.1.1.6**.

12   **Figure 3.5** and references thereto are renumbered **3.2.1.1.7-1**.

13   **Figure 3.6** and references thereto are renumbered **3.2.1.1.7-2**.

14   **Figure 3.7** and references thereto are renumbered **3.2.1.1.7-3**.

15   **Figure 3.8** and references thereto are renumbered **3.2.1.1.8**.

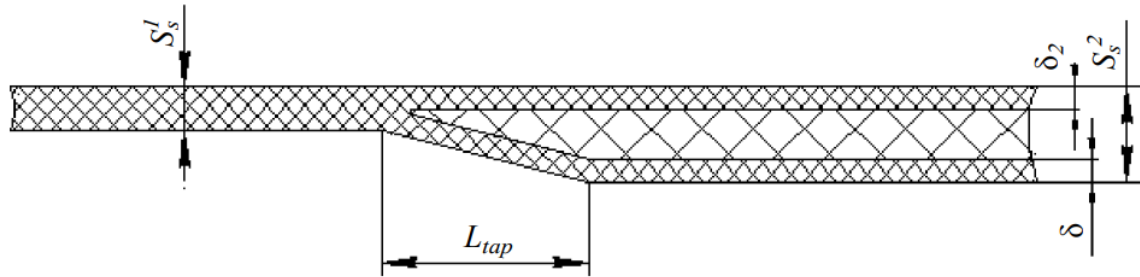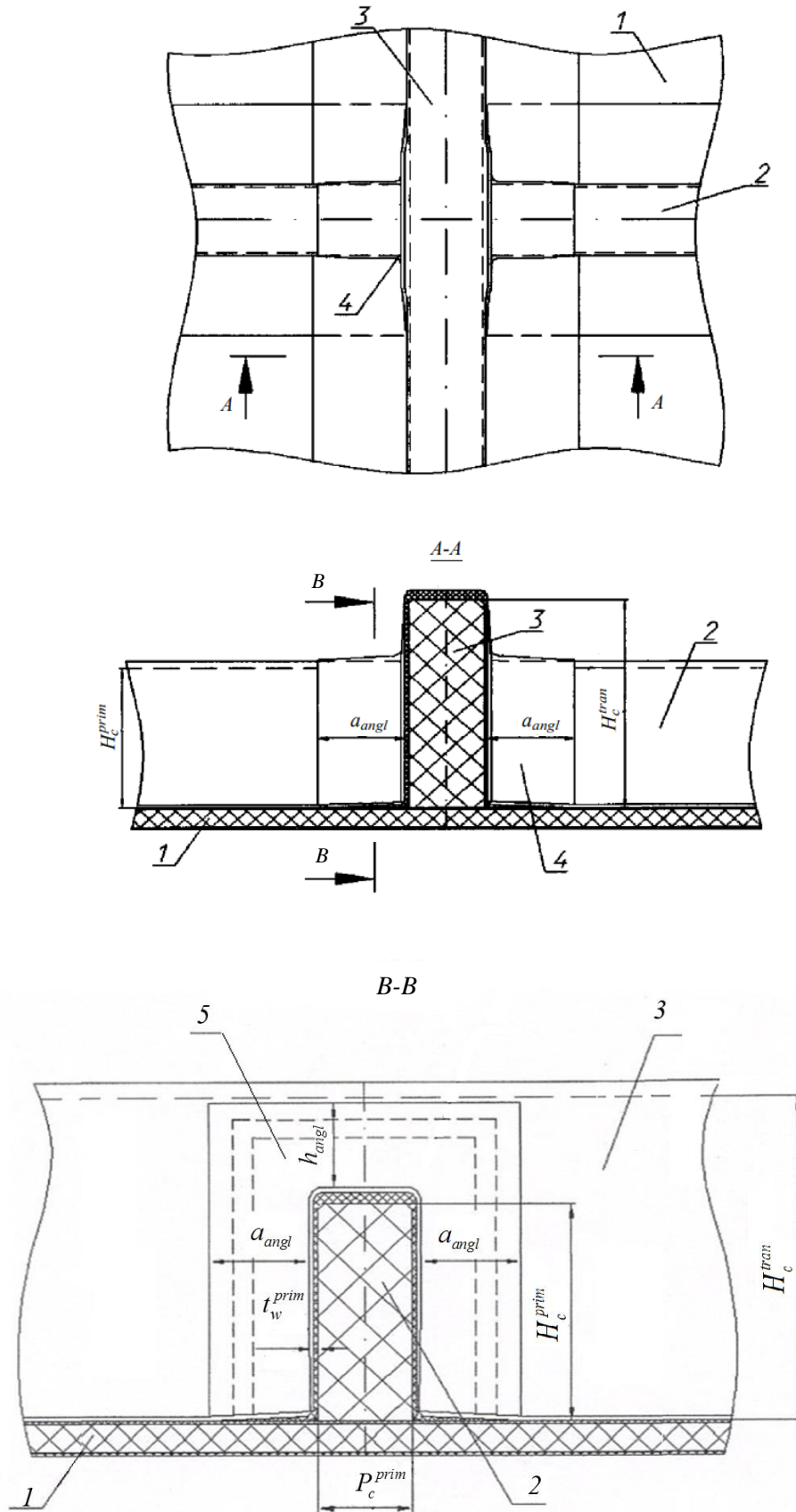16   **Figure 3.2.1.1.8** (former Figure 3.8) is replaced by the following one:

"

Fig. 3.2.1.18
Structure of a ship hull single-skin shell where its thickness varies".

17   **Figure 3.9** and references thereto are renumbered **3.2.1.2.4-1**.

18   **Figure 3.10** and references thereto are renumbered **3.2.1.2.4-2**.

19   **Figure 3.11** and references thereto are renumbered **3.2.1.2.5**.

20   **Figure 3.12** and references thereto are renumbered **3.2.2.2.5**.

21   **Figure 3.13** and references thereto are renumbered **3.2.2.2.9**.

22   **Figure 3.2.2.2.9** (former Figure 3.13) is replaced by the following one:

"

Fig. 3.2.2.2.9
Single-skin to sandwich transition of the deck plating".

23   **Figure 3.14** and references thereto are renumbered **3.2.4.2.1**.

24   **Figure 3.15** and references thereto are renumbered **3.2.4.2.3**.

25   **Figure 3.16** and references thereto are renumbered **3.2.4.9**.

26   **Table 3.1** and references thereto are renumbered **3.2.4.13**.

27   **Figure 3.17** and references thereto are renumbered **3.2.4.15**.

28   **Figure 3.18** and references thereto are renumbered **3.2.4.16**.

Figure 3.2.4.16 (former Figure 3.18) is replaced by the following one:

"

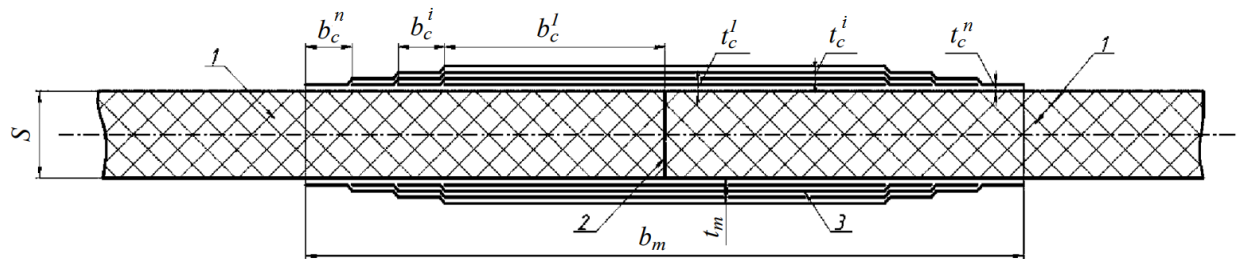Fig. 3.2.4.16
Intersection of closed box sections of different depths:
1 — shell (deck); *2* — longitudinal; *3* — transverse; *4* — angle straps; *5* — thickening of transverse webs:
$$a_{angl} \geq B_c^{prim}; \quad t_{angl} = 0,8 t_w^{prim}; \quad h_{angl} \cong (H_c^{tran} - H_c^{prim}) \leq a_{angl}\text{"}.$$

30   **Figure 3.19** and references thereto are renumbered **3.2.4.17**.

31   **Figure 3.20** and references thereto are renumbered **3.2.4.18**.

32   **Figure 3.21** and references thereto are renumbered **3.2.4.19**.

33   **Figure 3.22** and references thereto are renumbered **3.2.4.21**.

34   **Figure 3.23** and references thereto are renumbered **3.2.4.22**.

35   **Figure 3.24** and references thereto are renumbered **3.2.4.23**.

36   **Figure 3.25** and references thereto are renumbered **3.2.4.24**.

37   **Figure 3.26** and references thereto are renumbered **3.2.4.25**.

38   **Figure 3.27** and references thereto are renumbered **3.2.4.28**.

39   **Figure 3.28** and references thereto are renumbered **3.2.5.2-1**.

40   **Figure 3.29** and references thereto are renumbered **3.2.5.2-2**.

41   **Figure 3.30** and references thereto are renumbered **3.2.5.3**.

42   **Figure 3.31** and references thereto are renumbered **3.2.6.2.2**.

43   **Figure 3.2.6.2.2** (former Figure 3.31) is replaced by the following one:

"

Fig. 3.2.6.2.2
Structural scheme of a moulded butt (seam) joint of single-skin members without edge preparation:
1 — members being jointed; *2* — butt; *3* — straps".

44   **Para 3.2.6.2.2** is replaced by the following text:

"**.2**   where the thickness of single-skin members being jointed does not exceed 10 mm, edge preparation may be omitted (refer to Fig. 3.2.6.2.2).
For this type of joint, strap parameters shall be selected from the following:
$b_m \geq 180 + 15s$, in mm;
$b_c^{\,1} = 30 \div 50$, in mm — half width of the first fiber layer of the strap;
$b_c^i = 15 \div 25$, in mm — step width;
$b_c^n = 40 \div 50$, in mm — width of the last *n*-th step of the strap;
$t_m \geq 0{,}5s$, in mm — for butt straps with parallel reinforcement scheme (0°/90°);
$t_m \geq 0{,}8s$, in mm — for butt straps with parallel and diagonal reinforcement scheme (0°/90°)(+45°/–45°);
$t_c^{\,1}, t_c^i, t_c^n$ — step height equal to the total thickness of the fiber layers forming the step.".

45   **Figure 3.32** and references thereto are renumbered **3.2.6.2.4**.

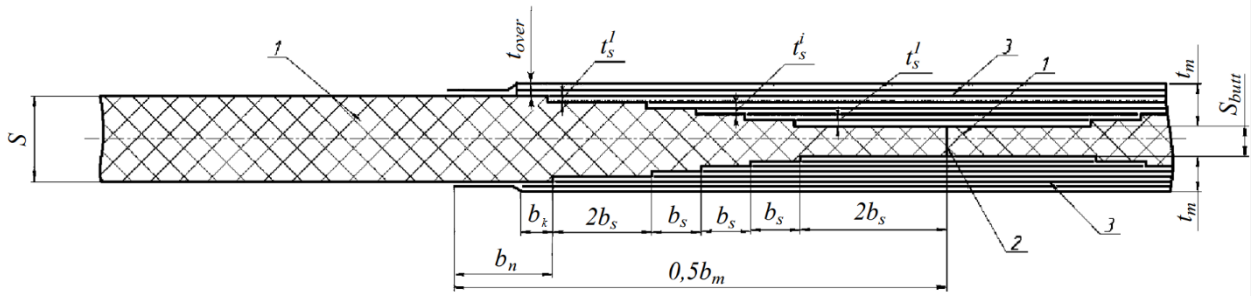46   **Figure 3.2.6.2.4** (former Figure 3.32) is replaced by the following one:

"

Fig. 3.2.6.2.4
Structural scheme of a moulded butt (seam) joint of single-skin members with double side stepped edge preparation:
1 — members being jointed; *2* — butt; *3* — straps".

47   **Para 3.2.6.2.4**. The next to the last and the last paragraphs are replaced by the following text:

"Joint parameters for single-skin members shall be selected from the following:
$S_{butt} = m'''_{butt} \cdot t_d$, in mm;
$m'''_{butt} \geq 2$;
$n_1 = m''' - m'''_{butt}$;
m''' = number of fabric layers in load-bearing layer;
m'''_{butt} = number of fabric layers in the butt of load-bearing layer;
$n_2 = (n_1 - 6)/3$ (where n_2 is a fractional number, it is rounded to the smallest integral value);
$t_m > \delta_{imax}$, in mm,
where δ_{imax} $(i = 1,2)$ = maximum thickness of one of two load-bearing layers;
S_{butt} = thickness of load-bearing layers in the butt.
Other strap parameters, number of steps and their depth shall be determined from the above correlations for the stepped joint of single-skin members;".

48   **Figure 3.33** and references thereto are renumbered **3.2.6.2.5**.

49   **Figure 3.2.6.2.5** (former Figure 3.33) is replaced by the following one:

"

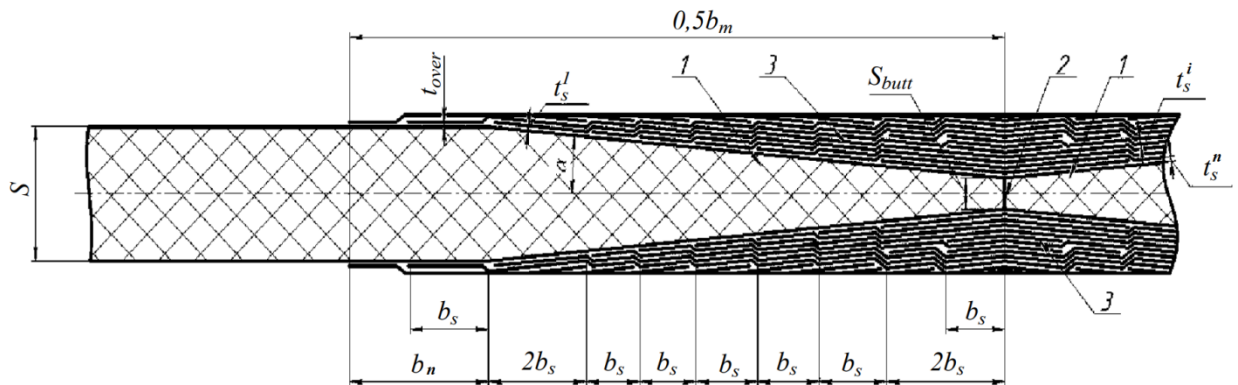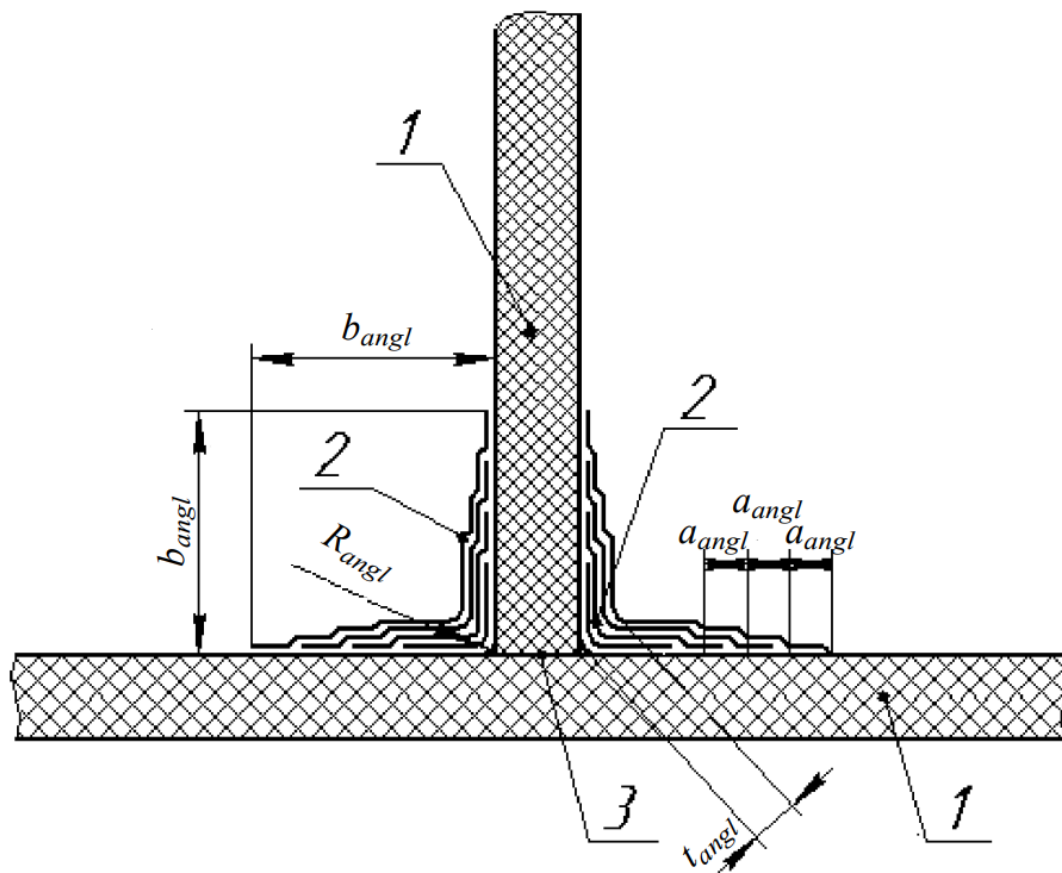
Fig. 3.2.6.2.5
Structural scheme of a moulded butt (seam) joint of single-skin members with double stepped beveling:
1 — members being connected; *2* — butt; *3* — straps".

50　　**Para 3.2.6.2.5**. The definition of the parameter b_c after the sentence "Parameters of butt joint with beveling for single-skin members shall be selected from the following:" is replaced by the following text:

"$b_s = 15 \div 20$, mm".

51　　**Para 3.2.6.3.2**. Dimension "mm" is added to the parameter "s":

"where $s =$ thickness of a horizontal member, in mm;".

52　　**Figure 3.34** and references thereto are renumbered **3.2.6.3.2**.

53　　**Figure 3.2.6.3.2** (former Figure 3.34) is replaced by the following one:

"

Fig. 3.2.6.3.2
Structural scheme of a moulded fillet joint:
1 — members being jointed; *2* — moulding-in angles; *3* — contact surface".

54　　**Para 3.2.6.3.4** is replaced by the following text:

"**.4**　　for a stressed fillet joint, a horizontal single-skin member may be thickened under a vertical member, which may be both single-skin and sandwich, e.g. joint of a single-skin hull shell with a sandwich bulkhead. The foam plastic in core of the bulkhead in the area of joint with single-skin shell shall be replaced by that of the density increased by $30 \div 40$ kg/m^3 (but not more than 200 kg/m^3) in the form of embedded elements of certain scantlings (refer to Fig. 3.2.6.3.4).
　　The shell is thickened by adding fiber layers (woven roving or biaxial fabric with (0°/90°) reinforcement) between basic layers along the vertical member (across the hull). Thickness of the

thickened area shall taper towards edges, with each next fabric layer overlapping the preceding one with 20 — 25 mm increment. Thickened area scantlings shall be determined from the following:

$t_{th} = (0{,}2 \div 0{,}3)S_{shell};$

$B_{th} \geq 2(b_{th} + 6t_{th}) + S_{bulk}, \; b_{th} = b_{angl} + 5 \text{ mm};$

$b_{angl} \geq 16t_{angl}, \; t_{angl} \geq 0{,}6s_p,$

where $s_p = \max(S_{shell}, S_{bulk})$ — for connection of single-skin members;

$S_p = \max(S_{shell}, \delta_{bulk} + \delta_{bulk})$ — for connection of a single-skin and a sandwich members;

δ_{bulk} = thickness of the load-bearing layer of sandwich member;

$R_{angl} = 2t_{angl};$

$l_{angl}^{bulk} = 1{,}2\, S_{bulk};".$

55   **Figure 3.35** and references thereto are renumbered **3.2.6.3.4**.

56   **Figure 3.36** and references thereto are renumbered **3.2.6.3.5**.

57   **Figure 3.37** and references thereto are renumbered **3.2.6.3.7**.

58   **Figure 3.2.6.3.7** (former Figure 3.37) is replaced by the following one:
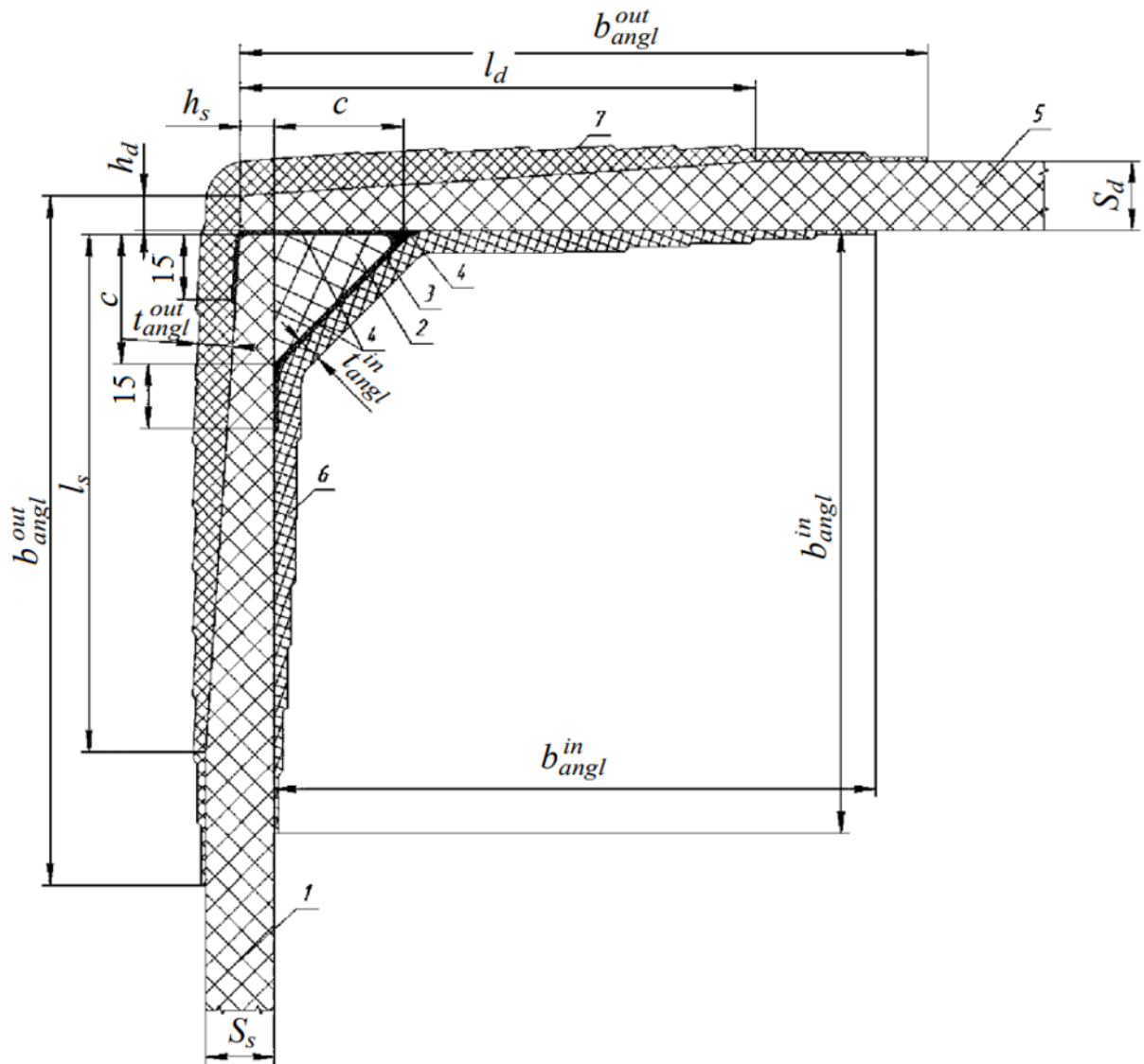
"

Fig. 3.2.6.3.7

Joint of side and upper deck single-skin constructions of variable thickness, with a support element installed:
1 — side; *2* — support element; *3* — support element sheathing; *4* — adhesive; *5* — upper deck plating;
6 — inner moulding-in angle; *7* — outer moulding-in angle".

59   **Figure 3.38** and references thereto are renumbered **3.2.6.3.8-1**.

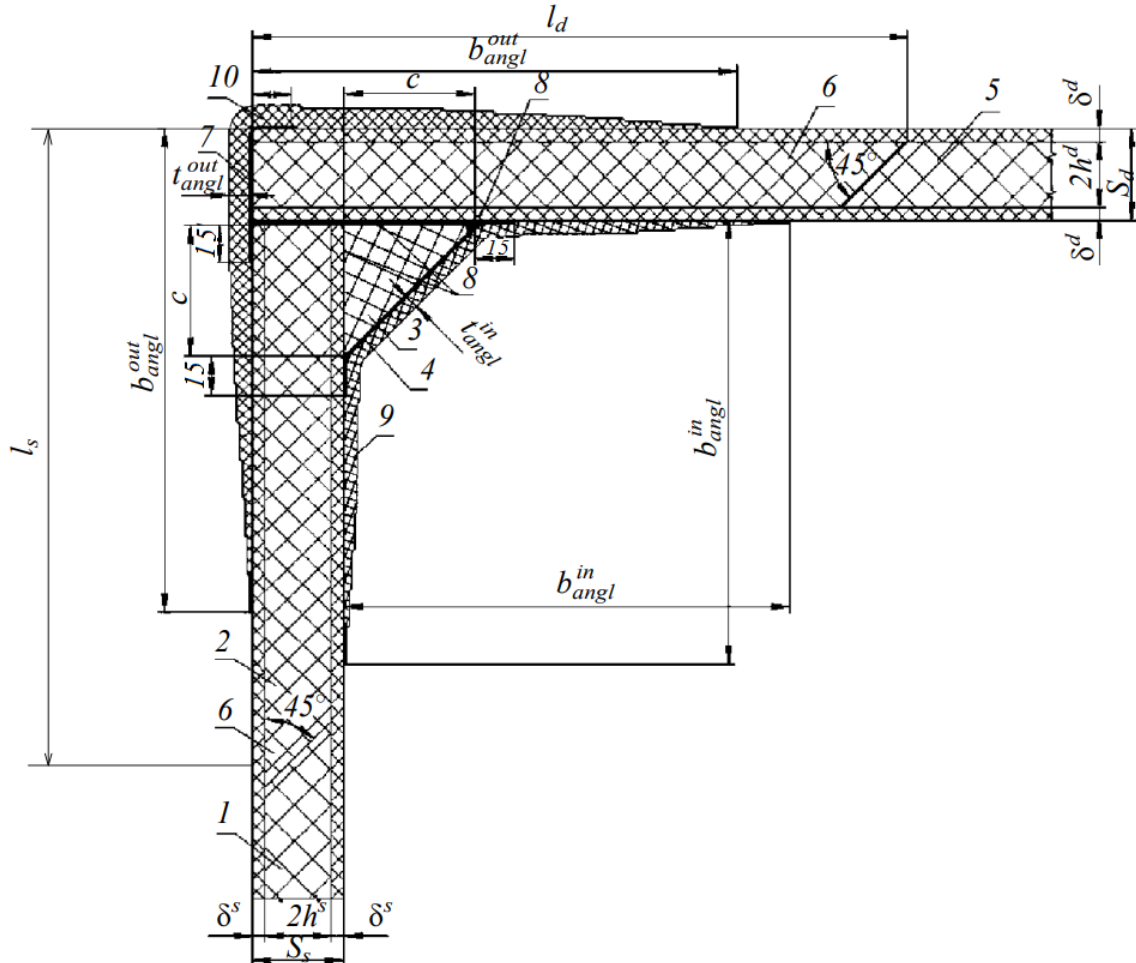60   **Figure 3.2.6.3.8-1** (former Figure 3.38) is replaced by the following:

"

Fig. 3.2.6.3.8-1
Joint of the upper deck plating and side plating of sandwich construction (Type A):
1 — side laminate; *2* — reinforcement of the foam plastic of increased density; *3* — support element; *4* — sheathing;
5 — deck laminate; *6* — reinforcement of the foam plastic of increased density; *7* — sheathing; *8* — adhesive;
9 — inner moulding-in angle; *10* — outer moulding-in angle".

61   **Figure 3.39** and references thereto are renumbered **3.2.6.3.8-2**.

62   **Para 3.2.6.3.9**. The next to the last paragraph is replaced by the following text:

"Basic parameters of these joints shall be selected from the following:
$c \geq 1{,}2\max(s_s, s_d)$; $t_{angl} \geq 0{,}4s_s$ or $t_{angl} \geq 2\delta^s$ (for the sandwich shell);
$b_{angl} \geq 15t_{angl} + c \geq 2s_s$.".

63   **Figure 3.40** and references thereto are renumbered **3.2.6.3.9-1**.

64   **Figure 3.41** and references thereto are renumbered **3.2.6.3.9-2**.

65   **Figure 3.42** and references thereto are renumbered **3.2.7.5**.

66   **Figure 3.43** and references thereto are renumbered **3.2.7.6-1**.

67   **Figure 3.44** and references thereto are renumbered **3.2.7.6-2**.

68   **Figure 3.45** and references thereto are renumbered **3.2.7.6-3**.

69   **Figure 3.46** and references thereto are renumbered **3.2.8.7-1**.

70   **Figure 3.47** and references thereto are renumbered **3.2.8.7-2**.

71   **Figure 3.48** and references thereto are renumbered **3.2.8.7-3**.

72   **Figure 3.49** and references thereto are renumbered **3.2.8.7-4**.

73   **Figure 3.50** and references thereto are renumbered **3.3.2.12-1**.

74   **Figure 3.51** and references thereto are renumbered **3.3.2.12-2**.

75   **Figure 3.52** and references thereto are renumbered **3.3.3.2**.

76   **Figure 3.53** and references thereto are renumbered **3.3.3.3-1**.

77   **Figure 3.54** and references thereto are renumbered **3.3.3.3-2**.

78   **Figure 3.3.3.3-2** (former Figure 3.54) is replaced by the following one:
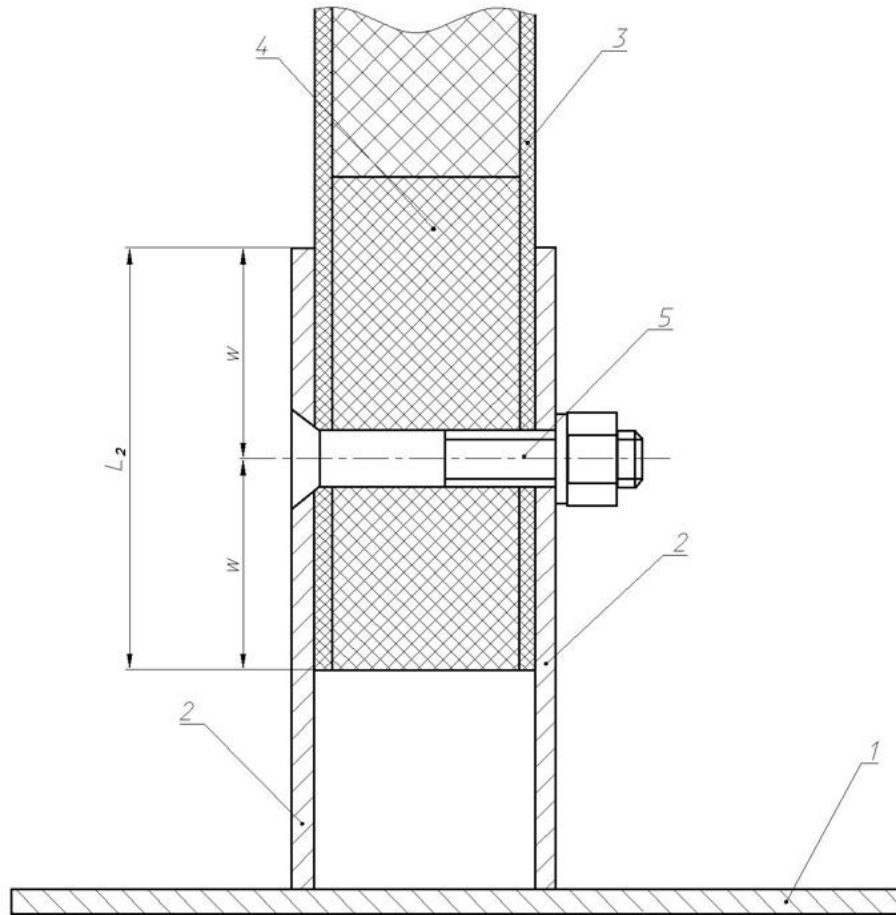
"

Fig. 3.3.3.3-2
Bonded and bolted joint of the bulkhead to the metal hull (with two metal coamings):
1 — hull deck; *2* — coamings; *3* — bulkhead; *4* — foam plastic of increased density; *5* — bolt".

4 HULLS OF BOATS AND MOTORBOATS

79   **Figure 4.1** and references thereto are renumbered **4.2.1**.

5 HULL STRENGTH AND SUPERSTRUCTURES

80   **Table 5.1** and references thereto are renumbered **5.3.4**.

81   **Table 5.2** and references thereto are renumbered **5.3.7**.

82   **Figure 5.1** and references thereto are renumbered **5.4.7**.

83   **Figure 5.2** and references thereto are renumbered **5.4.10**.

LONGITUDINAL AND BUCKLING STRENGTH OF HULL STRUCTURAL MEMBERS AND PLATES

(Recommendations on calculation)

1 STRESS-STRAIN BEHAVIOR OF FRAMING MEMBERS

84 **Figure 1** and references thereto are renumbered **1.1**.

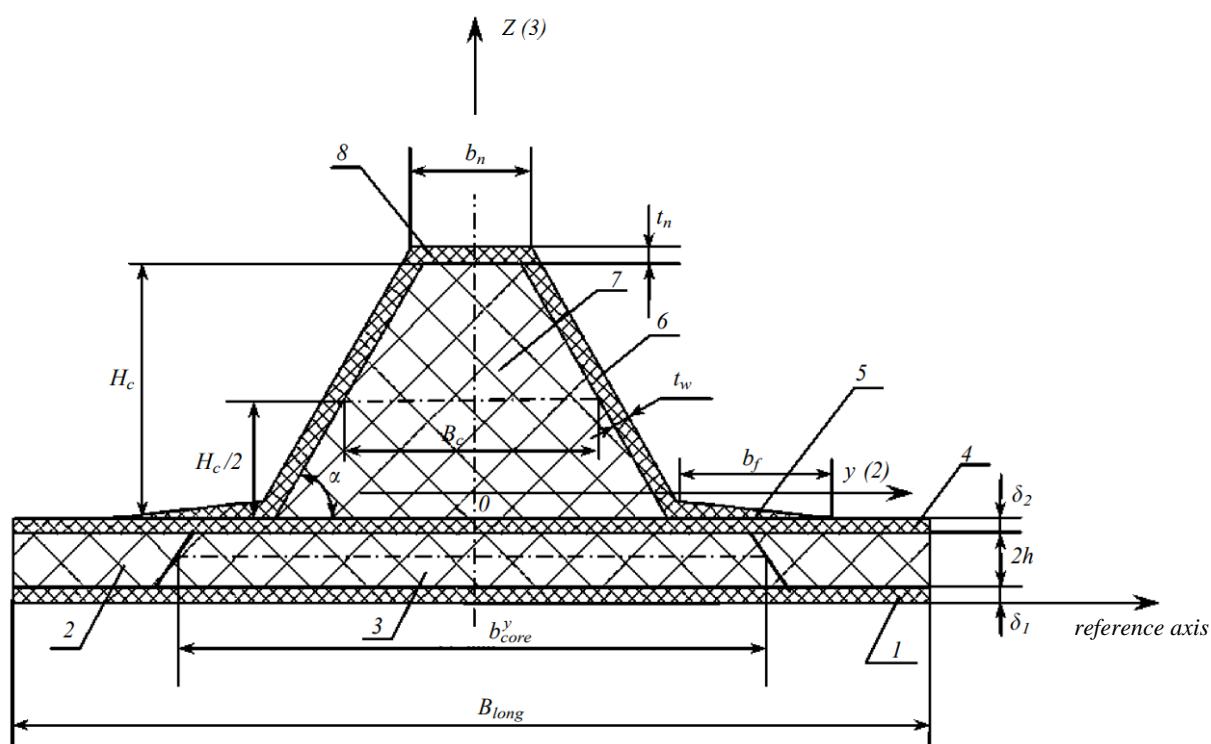85 **Figure 1.1** (former Figure 1) is replaced by the following one:

"

Fig. 1.1
Calculation method for the closed box (trapezoidal) member:
1, 4 — load-bearing layers; *2* — core; *3* — reinforcement with a core of increased density; *5* — flange; *6* — member web; *7* — core of a member; *8* — attached plate".

86 **Para 1.1** is supplemented by the following text:

"The member cross-section shear stiffness is determined by the formula

$$K_{11} = (2G_{13}^w t_w + G^c B_c)H$$

where $H = H_c + t_n$.".

87 **Figure 2** and references thereto are renumbered **1.3**.

88 **Table 1** and references thereto are renumbered **1.1**.

2 BUCKLING STRENGTH OF FRAMING MEMBERS

89 **Para 2.1**. The formula for determination of K_{11} is deleted.

90 **Para 2.2** is supplemented by the following text:

"l = member span, distance between member support sections.".

3 SHEAR STRESS-STRAIN BEHAVIOR OF SINGLE-SKIN PLATES

91 **Section 3** is replaced by the following text:

"Shear strain-stress behavior of single-skin plates shall be determined by the following formulae:

$$w = k_1 \frac{pb^4}{E_1 t^3};$$

$$M_1 = k_2 pb^2;$$

$$M_2 = k_3 pb^2;$$

$$M_2' = k_5 pb^2,$$

where p = design uniformly distributed load intensity;
M_1 = bending moment at the plate center in the section parallel to axis y per unit length of the section;
M_2 = bending moment at the laminate center in the section parallel to axis x per unit length of the section;
M_2' = bending moment in the middle of the longer side of the supporting contour in the section parallel to axis x per unit length of the section;
E_1 and E_2 = Young's moduli of the load-bearing layer in the direction of main reinforcement (direction 0°) and in the direction 90° to the main reinforcement;
t = plate thickness.

Values of factors k_i for isotropic and orthotropic plates, with the Young's moduli ratio along the shorter and longer sides of the plate equal to 1,0 and 1,5 are specified in Tables 3-1 and 3-2, for fixed bearing edges, and for plates with freely supported edges.
Where hull or deck platings are made with parallel and diagonal reinforcement schemes [(0°/90°)/(+45°/−45°)/(0°/90°)/……/(+45°/−45°)/(0°/90°)], plates shall be considered as isotropic ones with average values equal to a half-sum of the relevant characteristics in warp and weft directions of parallel layers:

$$E_{av} = \frac{E_1 + E_2}{2};$$
$$v_{av} = \frac{v_{12} + v_{21}}{2}.$$

where v_{12} and v_{21} = Poisson's ratios of the plate material (refer to Fig. 3).

The values specified for orthotropic plates refer to FRPs with parallel reinforcement schemes [(0°/90°)] (E_1/E_2 = 1,0; E_1/G_{12} = 5) and (E_1/E_2 = 1,5; E_1/G_{12} = 6), positioned with 1 – (0°) direction along the shorter side.
Maximum normal stresses in the plate are determined by the formula

$$\sigma_{ii} = \pm 6M_i / t^2.".$$

92 **Tables 2** and **3** and references thereto are renumbered **3-1** and **3-2** accordingly.

4 BUCKLING STRENGTH OF SINGLE-SKIN PLATES IN COMPRESSION

93 **Para 4.1** is replaced by the following text:

"**4.1** The buckling strength of freely supported single-skin plates in compression (Fig. 4.1) shall be determined with account of the aspect ratio of plate sides $\gamma = a/b$.
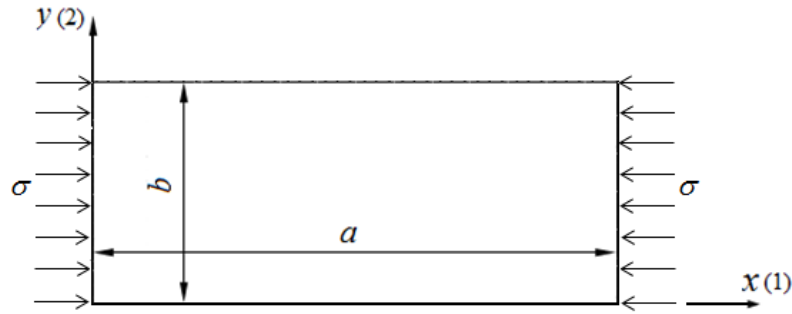

Fig. 4.1
Calculation method of single-skin plates in compression".

94 **Para 4.2** is replaced by the following text:

"**4.2 FRPs with parallel reinforcement scheme [(0º/90º)].**
Critical stress is determined by the formula

$$\sigma_{buck} = E_1 B (t/b)^2,$$

where E_1 = Young's compression modulus;
B = factor depending on the aspect ratio of plate sides;

$$B = \frac{(m/\gamma)^2 + 2\left[v_{21} + 2\frac{G_{12}}{E_1}(1 - v_{12}v_{21})\right] + \frac{E_2}{E_1}(\gamma/m)^2}{12(1 - v_{12}v_{21})} \pi^2,$$

where $\gamma = a/b$ — aspect ratio of plate sides;
m = number of half waves at buckling failure;
t = plate thickness;
E_1 and E_2 = Young's moduli in the direction of main reinforcement (direction 0°) and in the direction 90° to the main reinforcement;
G_{12} = shear modulus in the plate plane (refer to Fig. 4.1);
v_{12} and v_{21} = Poisson's ratios of the plate material (refer to Fig. 4.1).".

95 **Existing para 4.2** is renumbered **4.3**.

96 **Para 4.3** is replaced by the following text:

"**4.3 FRPs with parallel and diagonal reinforcement schemes [(0º/90º)/(+45º/−45º)/(0º/90º)/……/(+45º/−45º/(0º/90º)].**
When determining finite stiffness FRP plates with parallel and diagonal reinforcement scheme, the calculation method for relevant isotropic plates may be used. In such case, the average values of Young's modulus and Poisson's ratio shall be determined by the following formulae:

$$E_{av} = \frac{E_1 + E_2}{2};$$

$$v_{av} = \frac{v_{12} + v_{21}}{2}.$$

Critical stress is determined by the formula

$$\sigma_{buck} = E_{av} B (t/b)^2.$$

Values of factor B for $0{,}4 \leq \gamma \leq 3{,}0$ are specified in Table 4.3 and in Figs. 4.3-1 — 4.3-3.".

97   **Figures 4 — 6** and references thereto are renumbered **4.3-1 — 4.3-3** accordingly.

98   **Figures 4.3-1 — 4.3-3** (former Figures 4 —6). Symbols G_{12}^{bl} are replaced by G_{12} and symbols E_p^{bl} are replaced by E_1.

99   **Table 4** and references thereto are renumbered **4.3**.

100   **Table 4.3** (former Table 4). Symbols G_{12}^{bl} are replaced by G_{12} and symbols E_p^{bl} are replaced by E_1.

5 SHEAR BUCKLING STRENGTH OF SINGLE-SKIN PLATES

101   **Para 5.1** is replaced by the following text:

"**5.1**   The buckling strength of freely supported single-skin plates (Fig. 5.1) for shear stress of FRPs with parallel reinforcement scheme [(0%90°)] shall be determined with account of the aspect ratio of plate sides $\gamma = a/b$.
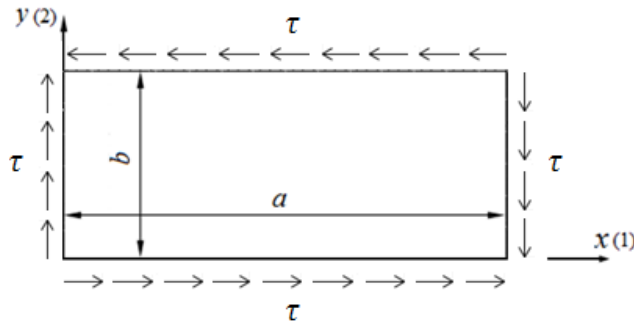

Fig. 5.1
Calculation method of single-skin plates under shear".

102   **Existing paras 5.1.1** and **5.1.2** are renumbered **5.2** and **5.3** accordingly.

103   **Para 5.2** is replaced by the following text.

"**5.2**   At $\gamma \geq 1$ the shear critical stress is determined by the formula

$$\tau_{buck} = (E_1/\gamma^4 + 2E_3/\gamma^4 + E_2)B(t/b)^2,$$

where $E_3 = E_1 v_{21} + 2(1 - v_{12}v_{21})G_{12}$;

$$B = \frac{\pi^4 \gamma}{384(1 - v_{12}v_{21})}\sqrt{\frac{100}{1{,}395 + 4(k_1 + k_2)}};$$

where $k_1 = \frac{1 + 2\gamma^2 A + \gamma^4 \xi}{81 + 18\gamma^2 A + \gamma^4 \xi}; k_2 = \frac{1 + 2\gamma^2 A + \gamma^4 \xi}{1 + 18\gamma^2 A + 81\gamma^4 \xi};$

$A = v_{21} + 2\frac{G_{12}}{E_1}(1 - v_{12}v_{21}); \gamma = {}^{a}/_{b}; \xi = \frac{E_2}{E_1};$

E_1, E_2, G_{12}, v_{12} and v_{21} — refer to 4.

N o t e . Reinforcement direction (0°) — along side of length a (refer to Fig. 5.1).

Values of factor B for $\gamma \geq 1$ are specified in Table 5.2 and in Fig. 5.2;".

104   **Table 5** and references thereto are renumbered **5.2**.

105   **Table 5.2** (former Table 5). Symbols G_{12}^{bl} are replaced by G_{12} and symbols E_p^{bl} are replaced by E_1.

106   **Figure 7** and references thereto are renumbered **5.2**.

107   **Figure 5.2** (former Figure 7). Symbols G_{12}^{bl} are replaced by G_{12} and symbols E_p^{bl} are replaced by E_1.

108   **Para 5.3** is replaced by the following text:

"**5.3**   At $\gamma = 0{,}5$ the shear critical stress is determined by the formula

$$\tau_{buck} = B\left({^t}\!/_b\right)^2,$$

where $B = 0{,}00952 \dfrac{\pi^4}{1-\nu_{12}\nu_{21}} \sqrt{D - \sqrt{D^2 - 9{,}58C}};$

where $C = E'\bar{E} \cdot \hat{E} \cdot \tilde{E};$
$D = 4{,}82E'\bar{E} + 1{,}31E'\tilde{E} + 0{,}64\hat{E} \cdot \tilde{E} + 0{,}101\bar{E} \cdot \tilde{E};$
$E' = E_1 + 2E_3 + E_2;$
$\bar{E} = 16E_1 + 18E_3 + 5{,}06E_2;$
$\hat{E} = E_1 + 8E_3 + 16E_2;$
$\tilde{E} = 16E_1 + 50E_3 + 39E_2.$

Values of factor B for $\gamma = 0{,}5$ are specified in Table 5.3 and in Fig. 5.3.".

109   **Table 6** and references thereto are renumbered **5.3**.

110   **Table 5.3** (former Table 6). Symbols G_{12}^{bl} are replaced by G_{12} and symbols E_p^{bl} are replaced by E_1.

111   **Figure 8** and references thereto are renumbered **5.3**.

112   **Figure 5.3** (former Figure 8). Symbols G_{12}^{bl} are replaced by G_{12} and symbols E_p^{bl} are replaced by E_1.

113   **Figure 5.3** (former Figure 8). Dimension "E_1, GPa" is added to axis x.

6 STRESS-STRAIN BEHAVIOR OF SANDWICH PLATES AT CYLINDRICAL BENDING

114   **Section 6** is replaced by the following text:

"This Section contains the formulae to determine maximum deflections, maximum normal stresses in load-bearing layers and maximum shear stresses in the core for sandwich plates with isotropic core of the FRP hull structures.

Transverse deflection of cylindrical plate bending taking into account various modes of plate edge attachment (Fig. 6) where $\gamma = {^a}\!/_b > 3$ is considered. In all cases, the load shall be perpendicular to the plate plane.
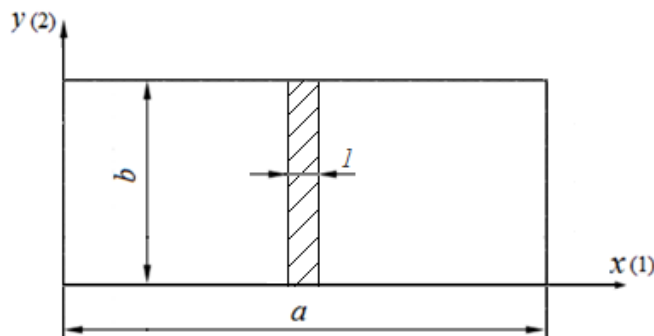
Fig. 6
Cylindrical bending of sandwich plates

Symbols.

For the purpose of this Section, the following symbols have been adopted:

δ = thickness of each load-bearing layer, in m;

h = half thickness of the sandwich plate core, in m;

E_{ll} = Young's modulus of load-bearing layers made of isotropic material, in Pa;

G_{ll} = shear modulus in plane of load-bearing layers, in Pa;

μ_{ll} = Poisson's ratio of load-bearing layers;

E_{core} = Young's modulus of the isotropic core, in Pa;

G_{core} = shear modulus of the isotropic core, in Pa;

μ_{core} = Poisson's ratio of the isotropic core;

q = uniformly distributed transverse load per surface area, in N/m²;

p = uniformly distributed transverse load per unit length, in N/m;

W = maximum deflection of load-bearing layers of the plate, in m;

σ_x = maximum normal stresses in load-bearing layers, in Pa;

τ_{xz} = maximum shear stresses in the isotropic core, in Pa.

Where load-bearing layers are made of the same isotropic material and have the same thickness, the following conditions shall be met:

$$E_i^1 = E_i^2 = E_{ll}, \ \mu_{ij}^1 = \mu_{ij}^2 = \mu_{ll}, \ \delta_1 = \delta_2 = \delta,$$

where $i, j = 1, 2, 3$ — directions of coordinate axes;
E_i^1, E_i^2 = Young's moduli of load-bearing layers;
μ_{ij}^1, μ_{ij}^2 = Poisson's ratios of load-bearing layers;
δ_1, δ_2 = thicknesses of load-bearing layers.

For the core made of isotropic material, the following conditions shall be met:

$$E_i^{core} = E_{core}, \mu_{ij} = \mu_{core},$$

where E_i^{core} = Young's modulus of the core;
μ_{ij} = Poisson's ratio of the core.

The formulae specified in this Section may be used where the following conditions are met:

$$2{,}0 \cdot 10^{-4} \le {G_{core}}/{\bar{E}} \le 2{,}0 \cdot 10^{-2}, \ 0{,}1 \le {\delta}/{h} \le 0{,}25,$$

where $\bar{E} = {E_{ll}}/{(1 - \mu_{ll}^2)}.$

The formulae may be used for calculation of sandwich plates with orthotropic load-bearing layers, where their Young's moduli do not vary more than 20 % (relative to the highest value of the moduli), i.e. if the following condition is met:

$$(1 - {E_2}/{E_1}) \cdot 100 < 20 \ \% \ \text{ at } E_1 > E_2,$$

where E_1 and $E_2 = $ Young's moduli of the load-bearing layer in the direction of main reinforcement (direction 0°) and in the direction 90° to the main reinforcement.

In this case, the arithmetic mean shall be taken as the Young's modulus for calculations. The values used in the formulae specified in Table 6 are determined by the following formulae:

$$B_{ll} = \frac{E_{ll}\delta}{1-\mu_{ll}^2}, \ B_{core} = \frac{2E_{core}h}{1-\mu_{core}^2}, \ D_{ll} = \frac{E_{ll}\delta^3}{12(1-\mu_{ll}^2)}, \ D_{core} = B_{core}\frac{h^2}{3},$$

$$k = \frac{\pi^2 B_{ll}h_{long}}{G_{core}a^2}, \ \gamma = \frac{\pi}{a}\sqrt{1/\left(k\frac{2D_{ll}\eta}{D_{pl}}\right)}, \ h_{long} = h\left(1 + \frac{D_{core}}{2B_{ll}h^2}\right),$$

$$\eta = 1 + \frac{D_{core}\delta^2}{8h_{long}hD_{ll}}, \quad D_{pl} = 2(D_{ll} + B_{ll}(h + \delta/2)^2) + D_{core}, \quad \bar{E} = \frac{E_{ll}}{1-\mu_{ll}^2}.".$$

115   **Table 7** and references thereto are renumbered **6**.

116   **Table 6** (former Table 7). Formulae for factors m_2 and m_3 in column "Stresses" for the type of load "Plate edges are freely supported, the transverse load is uniformly distributed" are replaced by the following ones:

$$"m_2 = 1 - \frac{4k}{\pi^2}\left(\frac{\delta}{h_{long}} + \frac{4D_{ll}\eta}{D_{pl}} - \frac{2+\delta/h_{long}}{1+\delta/h} \times (\frac{\delta}{h} + [\frac{2D_{ll}}{D_{pl}}(1 - \frac{D_{core}\delta}{4hD_{ll}}) - \frac{\delta}{h(2+\delta/h_{long})}(1 - \frac{2D_{ll}\eta}{D_{pl}})]\text{sch}(\frac{\gamma a}{2}))),$$
$$m_3 = (1 - \frac{2D_{ll}\eta}{D_{pl}})(1 - \frac{4 \cdot k}{\pi^2} \cdot \frac{2 \cdot D_{ll} \cdot \eta}{D_{pl}} \cdot \frac{\gamma \cdot a}{2} \cdot th(\frac{\gamma \cdot a}{2})).".$$

117   **Table 6** (former Table 7). The first paragraph and formula in column "Deflections" for the type of load "Plate edges are freely supported, the transverse load is uniformly distributed" are replaced by the following text:

"Plate deflection is maximum in the section at $x = a/2$:
$$|W| = \left|\frac{5}{384} \cdot \frac{qa^4}{D_{pl}} m_1\right|,".$$

118   **Table 6** (former Table 7). The formula in column "Stresses" for the type of load " Plate edges are freely supported, the transverse load is uniformly distributed in the center section" is replaced by the following one:

$$"|\sigma_x| = \left|\frac{pa}{4} \cdot \frac{B_{ll}(h+\delta)}{\delta D_{pl}} m_2\right|,".$$

119   **Table 6** (former Table 7). The first paragraph in column "Stresses" for the type of load "Plate edges are fixed, the transverse load is uniformly distributed" is replaced by the following text:

"Normal stresses in load-bearing layers are maximum at $x = 0, a; z = \pm(h + \delta):".$

120   **Table 6** (former Table 7). The formula for factor m_1 in column "Deflections" for the type of load "Plate edges are fixed, the transverse load is uniformly distributed in the center section" is replaced by the following one:

$$"m_1 = 1 + \frac{48k}{\pi^2}\left(1 - \frac{2D_{ll}\eta}{D_{pl}}\right) \times \left(1 - \frac{4th(\gamma a/4)}{\gamma a}\right).".$$

121   **Table 6** (former Table 7). The formula for factor m_2 in column "Stresses" for the type of load "Plate edges are fixed, the transverse load is uniformly distributed in the center section" is replaced by the following one:

$$"m_2 = 1 - \frac{th(\gamma a/4)}{\eta(1+\delta/h)(\gamma a/4)} \times \left(\left(1 - \frac{D_{core}\delta}{4hD_{ll}}\right)\left(1 + \frac{\delta}{2h_{long}}\right) - \frac{\delta D_{pl}}{4hD_{ll}}\left(1 - \frac{2D_{ll}\eta}{D_{pl}}\right)\right),".$$

122   **Table 6** (former Table 7). The second inequality in columns "Stresses" and "Deflections" for the type of load "Plate edges are freely supported, the transverse load is uniformly distributed in the random section" is deleted.

123   **Table 6** (former Table 7). The formula for determination of the plate deflection for the type of load "Plate edges are freely supported, the transverse load is uniformly distributed in the random section" is replaced by the following one:

$$"|W| = |\frac{p}{D1_{pl}} \cdot \left[C_2 - C_1 \cdot x + C_3 \cdot \left(\frac{2 \cdot B_{ll} \cdot (h+\delta/2)}{G_{core}} - \frac{x^2}{3}\right) \cdot x - \frac{C_4 \cdot x^2}{2} + C_5 \cdot \text{sh}(k1 \cdot x) + C_6 \cdot \text{ch}(k1 \cdot x)\right]|".$$

124   **Table 6** (former Table 7). The formula for factor C_2 in column "Deflections" for the type of load "Plate edges are freely supported, the transverse load is uniformly distributed in the random section" is replaced by the following one:

$$"C_2 = \frac{a/2-\xi}{4}\left(\frac{2B_{ll}(h+\delta/2)^2}{D_{ll}k1^2} + \frac{\xi}{3}(a-\xi) + \frac{a^2}{6}\right),".$$

125   **Table 6** (former Table 7). The formula for factor C_6 in column "Deflections" for the type of load "Plate edges are freely supported, the transverse load is uniformly distributed in the random section" is replaced by the following one:

$$"C_6 = -\frac{B_{ll}(h+\delta/2)^2 \cdot sh(k1(a/2-\xi))}{2D_{ll}k1^3 \cdot ch(k1a/2)},".$$

126   **Table 6** (former Table 7). The last paragraph in column "Deflections" for the type of load "Plate edges are freely supported, the transverse load is uniformly distributed in the random section" is replaced by the following text:

"Plate deflection is maximum in the section, with coordinate $\partial W/\partial x = 0$ and within the range $-a/2 \le x \le \xi$;
(plate deflection at $x = \xi$ differs from the maximum value by not more than 10 %)".

127   **Table 6** (former Table 7). The formula for determination of tangential stresses in the core and preceding text in column "Stresses" for the type of load "Plate edges are freely supported, the transverse load is uniformly distributed in the random section" are replaced by the following text:

"tangential stresses in the core are maximal at $-a/2 \le x \le \xi$; $z = 0$ (at $\xi \le 0$):

$$|\tau_{xz}| = \frac{p}{D1_{pl}} \cdot 2B_{ll}(h+\delta/2)\left[C_3 + \frac{D_{ll}k1^3}{2B_{ll}(h+\delta/2)^2} \times \left(C_5 \cdot ch(-k1a/2) + C_6 \cdot sh(-k1a/2)\right)\right]|,".$$

128   **Table 6** (former Table 7). The formula for determination of normal stresses in load-bearing layers in column "Stresses" for the type of load "Laminate edges are free-standing, the transverse load is distributed according to the triangular law" is replaced by the following one:

$$"|\sigma_x| = \left|\frac{q_0 x_2}{2h+\delta} \times \left(\frac{2(h+\delta)}{\delta(2h+\delta)}\left(\frac{hB_{ll}}{G_{core}} + \frac{a^2-x_2^2}{6}\right) - \frac{hB_{ll}}{\delta G_{core}}\right)\right|,".$$

129   **Table 6** (former Table 7). The factor x_2 in the formula for determination of the plate deflection maximum value in column "Deflections" for the type of load "Laminate edges are free-standing, the transverse load is distributed according to the triangular law" is replaced by x_1.

130   **Table 6** (former Table 7). The formula for factor m_1 in column "Deflections" for the type of load "Laminate edges are free-standing, the transverse load is distributed according to the triangular law" is replaced by the following one:

$$"m_1 = \frac{q_0}{180B_{ll}(2h+\delta)^2},".$$

7 STRESS-STRAIN BEHAVIOR OF SANDWICH PLATES AT CYLINDRICAL BENDING EXPOSED TO LOCAL LOADS

131   **Section 7**. The first paragraph is replaced by the following text:

"This Section contains the formulae to determine maximum deflections, maximum normal stresses in load-bearing layers and maximum shear stresses in the core for sandwich plates with isotropic core of the FRP hull structures. The sandwich plate cylindrical bending (Fig. 6) when exposed to local loads is considered."

132 **Section 7**. The following explication is added to the formula $"(1 - E_2/E_1) \cdot 100 < 20\ \%$ at $E_1 > E_2"$:

"where E_1 and E_2 = Young's moduli of the load-bearing layer in the direction of main reinforcement (direction 0°) and in the direction 90° to the main reinforcement.".

133 **Section 7**. The inequality for determination of maximum normal stresses acting in the upper load-bearing layer of the plate is replaced by the following one:

$$"\sqrt[3]{E_{core}/E_{ll}} \cdot (2h/\delta) \leq 8{,}0;".$$

134 **Section 7**. The inequality for determination of maximum deflections of the plate is replaced by the following one:

$$"\sqrt[3]{E_{core}/E_{ll}} \cdot (2h/\delta) \leq 1{,}6.".$$

135 **Table 8** and references thereto are renumbered **7**.

136 **Table 7** (former Table 8). The formula for determination of plate deflection in column "Deflections" for the type of load "The plate is loaded with the moment uniformly distributed over the plate's width in any section" is replaced by the following one:

$$"|W| = \left| M \sqrt{\frac{3}{CE_{ll}\delta^3}}\, e^{-mx} \sin(mx) \right|,".$$

137 **Table 7** (former Table 8). The expressions for C_φ'' and C_β''' in the explication to formula in column "Stresses" for the type of load "The transverse load is uniformly distributed in the local region of the plate in any area" are replaced by the following ones:

$$"C_\varphi''' = -2 \cdot \big(\mathrm{sh}(\varphi) \cdot \cos(\varphi) + \mathrm{ch}(\varphi) \cdot \sin(\varphi)\big),$$
$$C_\beta''' = -2 \cdot \big(\mathrm{sh}(\beta) \cdot \cos(\beta) + \mathrm{ch}(\beta) \cdot \sin(\beta)\big),".$$

138 **Table 7** (former Table 8). The expression for C_β'' in the explication to formula in column "Deflections" for the type of load "The transverse load is uniformly distributed in the local region of the plate in any area" is replaced by the following one:

$$"C_\beta''' = -2 \cdot \big(\mathrm{sh}(\beta) \cdot \cos(\beta) + \mathrm{ch}(\beta) \cdot \sin(\beta)\big),".$$

139 **Table 7** (former Table 8). The common text in columns "Stresses" and "Deflections" for the type of load "The transverse load distributed according to the triangular law is applied in the local region of the plate in any area" is replaced by the following text:

"The distributed load value depending on the section coordinate is determined by the formula $q = q_{max}\,(x - a)/b$ in such case, parameter a shall be selected to meet the following condition: $20\delta \leq a \leq 30\delta.".$

140 **Table 7** (former Table 8). The expressions for C_φ''' and $C_{\alpha\beta}'''$ in the explication to formula in column "Stresses" for the type of load "The transverse load distributed according to the triangular law is applied in the local region of the plate in any area" are replaced by the following ones:

$$"C_\varphi''' = -2 \cdot \big(\mathrm{sh}(\varphi) \cdot \cos(\varphi) + \mathrm{ch}(\varphi) \cdot \sin(\varphi)\big),$$
$$C_{\alpha\beta}''' = -2 \cdot \big(\mathrm{sh}(\alpha + \beta) \cdot \cos(\alpha + \beta) + \mathrm{ch}(\alpha + \beta) \cdot \sin(\alpha + \beta)\big),".$$

141 **Table 7** (former Table 8). The expressions for C_φ''' and $C_{\alpha\beta}'''$ in the explication to formula in column "Deflections" for the type of load "The transverse load distributed according to the

triangular law is applied in the local region of the plate in any area" are replaced by the following ones:

$$"C_\varphi''' = -2 \cdot \left(\text{sh}(\varphi) \cdot \cos(\varphi) + \text{ch}(\varphi) \cdot \sin(\varphi)\right),$$
$$C_{\alpha\beta}''' = -2 \cdot \left(\text{sh}(\alpha + \beta) \cdot \cos(\alpha + \beta) + \text{ch}(\alpha + \beta) \cdot \sin(\alpha + \beta)\right),".$$

8 STRESS-STRAIN BEHAVIOR OF SANDWICH PLATES AT BENDING

142 **Para 8.1** is replaced by the following text:

"**8.1 Plate edges are freely supported, the transverse load is uniformly distributed.**
The formulae to determine maximum deflections, maximum normal stresses in load-bearing layers and maximum shear stresses in the core for symmetric sandwich plates with same thickness isotropic outer layers and transversally isotropic core with the isotropy plane matching the plate plane are given in 8.2. Transverse deflection of sandwich plates is considered. The load shall be perpendicular to the plate plane.
The formulae may also be used for calculation of plates with isotropic core.
S y m b o l s .
For the purpose of this Section, the following symbols have been adopted:
a = plate length, in m;
b = plate width, in m;
δ = thickness of each load-bearing layer, in m;
h = half thickness of the sandwich plate core, in m;
E_{bl} = Young's modulus of load-bearing layers in the sandwich plate, in Pa;
$\nu_{12(bl)}$ = Poisson's ratio of the material of load-bearing layers in the sandwich plate;
E_{core} = Young's modulus of core in isotropy plane of the sandwich plate, in Pa;
G_{core} = shear modulus of the core in plane that is orthogonal to the isotropy plane of the sandwich plate, in Pa;
ν_{core} = Poisson's ratio of the core of sandwich plate;
p = uniformly distributed load, in N/m²;
w = maximum deflection of load-bearing layers of the plate, in m;
σ_x, σ_y = maximum normal stresses in load-bearing layers, in Pa;
τ_{xz}, τ_{yz} = maximum shear stresses in the core, in Pa.
Calculations as per Formulae in 8.2 may be performed if the following conditions are met:

$$\frac{G_{core}}{E_{bl}}\left(1 - \nu_{12(bl)}^2\right) > 0{,}005 \text{ at } \frac{2h}{a}\sqrt{1 + \left(\frac{a}{b}\right)^2} \le 0{,}3 \text{ and } 0{,}01 \le \frac{\delta}{h} \le 0{,}5.$$
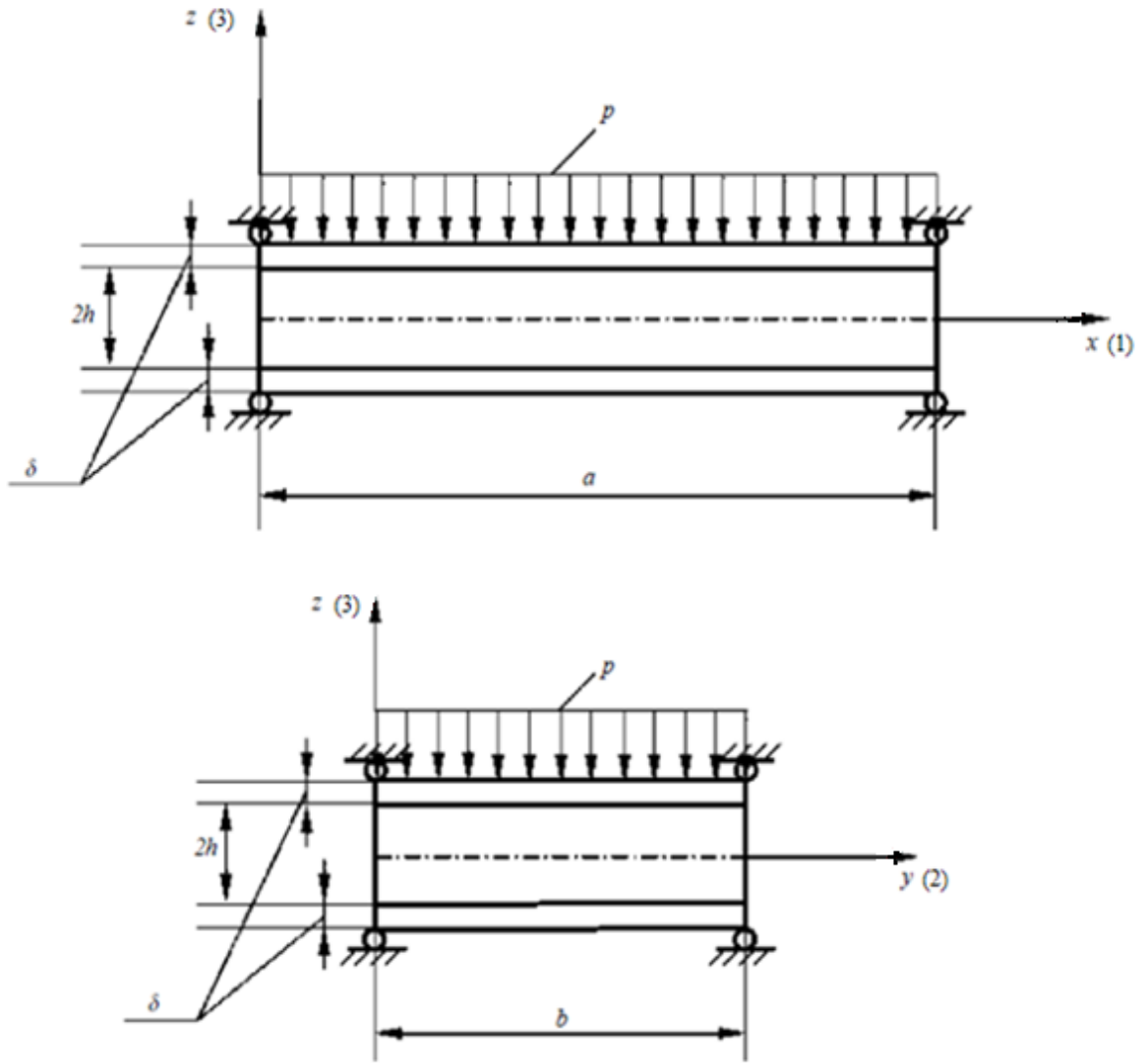
Fig. 8.1
Load type of the sandwich plate".

143   **Para 8.2** is replaced by the following text:

"**8.2**   Plate deflection is maximum at point $x = a/2$, $y = b/2$ and determined by the formula

$$|w|_{x=a/2,y=b/2} = \frac{8p}{\pi^2 G_{core}} m_1,$$

where $m_1 = \sum_{i=0}^{N}\sum_{j=0}^{N}(-1)^{(m-1)/2}(-1)^{(n-1)/2}\frac{1}{d \cdot m \cdot n \cdot r}\left(k_1 \text{ch}(r_1 h) + \frac{B_{ll} r}{G_{core}}\text{sh}(r_1 h)\right);$

$B_{ll} = \frac{E_{bl}\delta}{1-v_{12(bl)}^2};$

$2h =$ core thickness of the sandwich plate;

$m = 2i + 1, n = 2j + 1, \alpha = m\pi/a, b = n\pi/b;$

$r^2 = a^2 + \beta^2, r_1 = rk_1;$

$k_1 = \sqrt{\frac{E_{core}}{(1-v_{core}^2)\,G_{core}}};$

$d = \left(h + \frac{B_{ll}\delta^2 r^2}{3G_{core}}\right)r_1 \text{ch}(r_1 h) - \left(1 - \frac{B_{ll} r^2}{G_{core}}\left(h + \delta + \frac{B_{ll}\delta^2 r^2}{12G_{core}}\right)\right)\text{sh}(r_1 h).$

Normal stresses in load-bearing layers σ_x and σ_y are maximum at $x = a/2$, $y = b/2$ and determined by the following formulae:

$$\left.|\sigma_x|\right._{x=a/2,y=b/2} = \frac{8pE_{bl}}{(1-v_{12(bl)}^2)\pi^2 G_{core}} m_2,$$

$$m_2 = \sum_{i=0}^{N}\sum_{j=0}^{N}(-1)^{(m-1)/2}(-1)^{(n-1)/2}\frac{1}{d\cdot m\cdot n\cdot r^2}(\alpha^2 + v_{12(bl)}\beta^2)\left(\delta r_1 \mathrm{ch}(r_1 h) + \left(1 + \frac{B_{ll}\delta r^2}{2G_{core}}\right)\mathrm{sh}(r_1 h)\right);$$

$$\left.|\sigma_y|\right._{x=a/2,y=b/2} = \frac{8pE_{bl}}{(1-v_{12(bl)}^2)\pi^2 G_{core}} m_3,$$

$$m_3 = \sum_{i=0}^{N}\sum_{j=0}^{N}(-1)^{(m-1)/2}(-1)^{(n-1)/2}\frac{1}{d\cdot m\cdot n\cdot r^2}(\beta^2 + v_{12(bl)}\alpha^2)\left(\delta r_1 \mathrm{ch}(r_1 h) + \left(1 + \frac{B_{ll}\delta r^2}{2G_{core}}\right)\mathrm{sh}(r_1 h)\right).$$

Shear stresses in the core τ_{xz} are maximum at $x = 0; a, y = b/2$ and determined by the formula

$$\left.|\tau_{xz}|\right._{x=0;\, a,y=b/2} = \frac{8pB_{ll}}{\pi a G_{core}} m_4,$$

where $\quad m_4 = \sum_{i=0}^{N}\sum_{j=0}^{N}(-1)^{(n-1)/2}\frac{1}{d\cdot n}\cdot\left(\mathrm{sh}(r_1 h) + \frac{r_1\delta}{2} + \frac{r_1 G_{core}}{B_{ll}r^2}(\mathrm{ch}(r_1 h) - 1)\right).$

Shear stresses in the core τ_{yz} are maximum at $x = 0; a, y = b/2$ and determined by the formula

$$\left.|\tau_{yz}|\right._{x=a/2;\, y=0;b} = \frac{8pB_{ll}}{\pi b G_{core}} m_5,$$

where $\quad m_5 = \sum_{i=0}^{N}\sum_{j=0}^{N}(-1)^{(m-1)/2}\frac{1}{d\cdot m}\cdot\left(\mathrm{sh}(r_1 h) + \frac{r_1\delta}{2} + \frac{r_1 G_{core}}{B_{ll}r^2}(\mathrm{ch}(r_1 h) - 1)\right).$

N is taken so that the difference between values of neighboring terms of series does not exceed 5 %.

Values of factors m_i, $i = \overline{1,5}$ for sandwich plates with the most rational geometric and physical properties $h/\delta = 5$ and $v_{core} = 0{,}38 \div 0{,}4$ are specified in Figs. 8.2-1 — 8.2-15.

For other values of h/δ and v_{core}, factors m_i, $i = \overline{1,5}$ are determined by the formulae specified in this Section.

Values of γ and η are determined by the following formulae (refer to Figs. 8.2-1 — 8.2-15):

$$\gamma = a/b;$$

$$\eta = E_{bl}/E_{core}.".$$

144 **Figures 10 — 24** and references thereto are renumbered **8.2-1 — 8.2-15** accordingly.

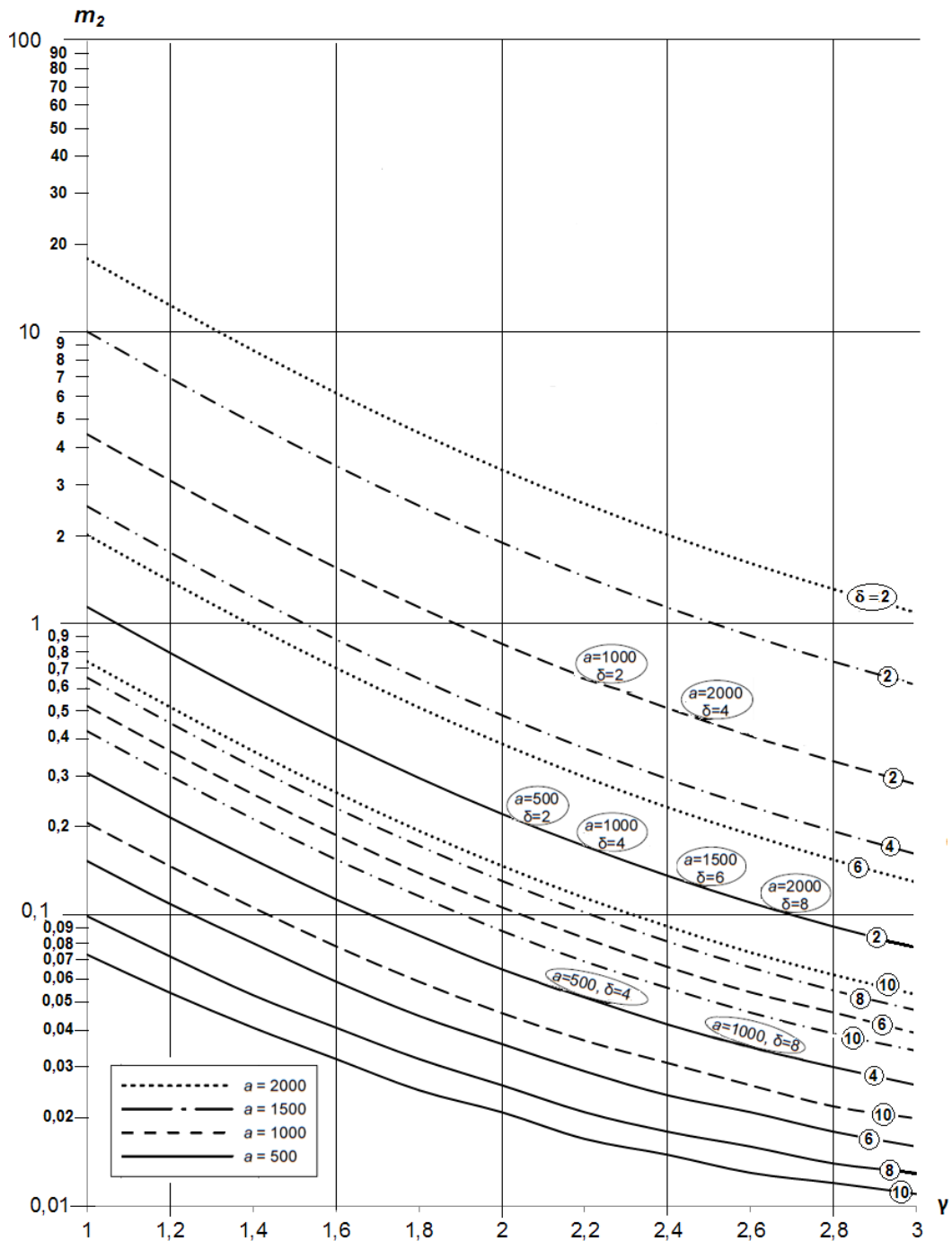145 **Figure 8.2-1** (former Figure 10). Dimension "m" is added to axis m_1.

146 **Figure 8.2-1** (former Figure 10). The caption of the figure is replaced by the following text:

" *Values of thickness δ, in mm, of the sandwich plate load-bearing layer are shown in circles*
Fig. 8.2-1
Values of factor m_1 at η = 100 for sandwich plates having length *a*, in mm"

147 **Figure 8.2-2** (former Figure 11). Dimension "m" is added to axis m_1.

148 **Figure 8.2-2** (former Figure 11). The caption of the figure is replaced by the following text:

" *Values of thickness δ, in mm, of the sandwich plate load-bearing layer are shown in circles*
Fig. 8.2-2
Values of factor m_1 at η = 400 for sandwich plates having length *a*, in mm".

149 **Figure 8.2-3** (former Figure 12). Dimension "m" is added to axis m_1.

150 **Figure 8.2-3** (former Figure 12). The caption of the figure is replaced by the following text:

151 **Figure 8.2-4** (former Figure 13) is replaced by the following one:
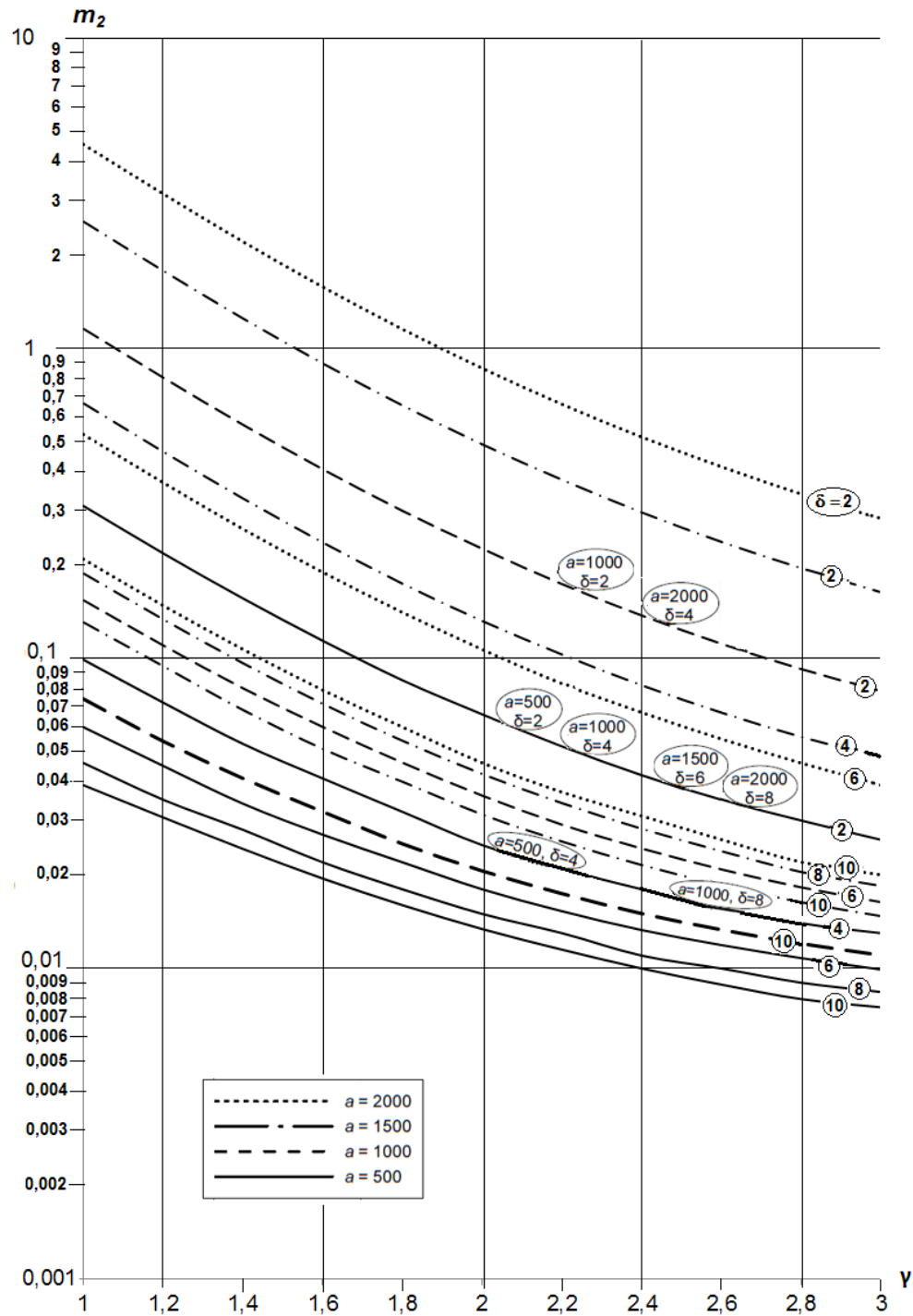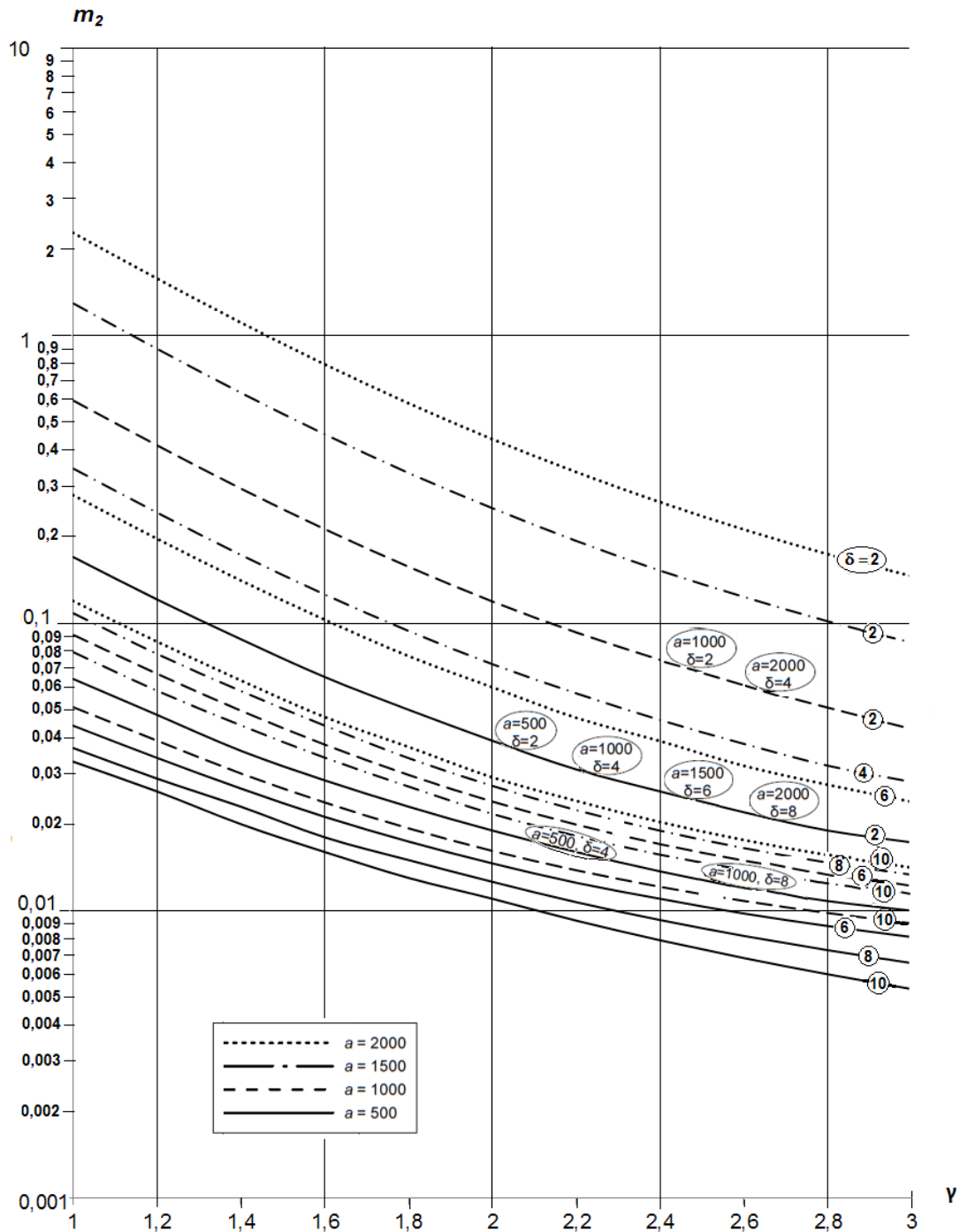
"

" *Values of thickness δ, in mm, of the sandwich plate load-bearing layer are shown in circles.*
Values of geometric properties of the sandwich plates for which diagrams of factor m_2 coincide in different
combinations of a and δ are shown in ovals
Fig. 8.2-4
Values of factor m_2 at η = 100 for sandwich plates of length *a*, in mm".

Figure 8.2-5 (former Figure 14) is replaced by the following one:

"

Values of thickness δ, in mm, of the sandwich plate load-bearing layer are shown in circles.
Values of geometric properties of the sandwich plates for which diagrams of factor m₂ coincide in different
combinations of a and δ are shown in ovals
Fig. 8.2-5
Values of factor m_2 at $\eta = 400$ for sandwich plates of length a, in mm".

153 **Figure 8.2-6** (former Figure 15) is replaced by the following one:

"

Values of thickness δ, in mm, of the sandwich plate load-bearing layer are shown in circles.
Values of geometric properties of the sandwich plates for which diagrams of factor m₂ coincide in different
combinations of a and δ are shown in ovals
Fig. 8.2-6
Values of factor m_2 at η = 800 for sandwich plates of length a, in mm".

154 **Figure 8.2-7** (former Figure 16). The caption of the figure is replaced by the following text:

"*Values of thickness δ, in mm, of the sandwich plate load-bearing layer are shown in circles.*
Values of geometric properties of the sandwich plates for which diagrams of factor m₃ coincide in different
combinations of a and δ are shown in ovals
Fig. 8.2-7
Values of factor m_3 at η = 100 for sandwich plates of length a, in mm".

155   **Figure 8.2-8** (former Figure 17). The caption of the figure is replaced by the following text:

"*Values of thickness δ, in mm, of the sandwich plate load-bearing layer are shown in circles.*
Values of geometric properties of the sandwich plates for which diagrams of factor m_3 coincide in different
combinations of a and δ are shown in ovals
Fig. 8.2-8
Values of factor m_3 at η = 400 for sandwich plates of length a, in mm".

156   **Figure 8.2-9** (former Figure 18). The caption of the figure is replaced by the following text:

"*Values of thickness δ, in mm, of the sandwich plate load-bearing layer are shown in circles.*
Values of geometric properties of the sandwich plates for which diagrams of factor m_3 coincide in different
combinations of a and δ are shown in ovals
Fig. 8.2-9
Values of factor m_3 at η = 800 for sandwich plates of length a, in mm".

157   **Figure 8.2-10** (former Figure 19). The caption of the figure is replaced by the following text:

"*Values of thickness δ, in mm, of the sandwich plate load-bearing layer are shown in circles.*
Values of geometric properties of the sandwich plates for which diagrams of factor m_4 coincide in different
combinations of a and δ are shown in ovals
Fig. 8.2-10
Values of factor m_4 at η = 100 for sandwich plates of length a, in mm".

158   **Figure 8.2-11** (former Figure 20). The caption of the figure is replaced by the following text:

"*Values of thickness δ, in mm, of the sandwich plate load-bearing layer are shown in circles.*
Values of geometric properties of the sandwich plates for which diagrams of factor m_4 coincide in different
combinations of a and δ are shown in ovals
Fig. 8.2-11
Values of factor m_4 at η = 400 for sandwich plates of length a, in mm".

159   **Figure 8.2-12** (former Figure 21). The caption of the figure is replaced by the following text:

"*Values of thickness δ, in mm, of the sandwich plate load-bearing layer are shown in circles.*
Values of geometric properties of the sandwich plates for which diagrams of factor m_4 coincide in different
combinations of a and δ are shown in ovals
Fig. 8.2-12
Values of factor m_4 at η = 800 for sandwich plates of length a, in mm".

160   **Figure 8.2-13** (former Figure 22). The caption of the figure is replaced by the following text:

"*Values of thickness δ, in mm, of the sandwich plate load-bearing layer are shown in circles.*
Values of geometric properties of the sandwich plates for which diagrams of factor m_5 coincide in different
combinations of a and δ are shown in ovals
Fig. 8.2-13
Values of factor m_5 at η = 100 for sandwich plates of length a, in mm".

161   **Figure 8.2-14** (former Figure 23). The caption of the figure is replaced by the following text:

"*Values of thickness δ, in mm, of the sandwich plate load-bearing layer are shown in circles.*
Values of geometric properties of the sandwich plates for which diagrams of factor m_5 coincide in different
combinations of a and δ are shown in ovals
Fig. 8.2-14
Values of factor m_5 at η = 400 for sandwich plates of length a, in mm".

162   **Figure 8.2-15** (former Figure 24). The caption of the figure is replaced by the following text:

"*Values of thickness δ, in mm, of the sandwich plate load-bearing layer are shown in circles.*
Values of geometric properties of the sandwich plates for which diagrams of factor m_5 coincide in different combinations of a and δ are shown in ovals
Fig. 8.2-15
Values of factor m_5 at η = 800 for sandwich plates of length *a*, in mm".

163   **Para 8.3** is replaced by the following text:

"**8.3   Plate edges are fixed along the supporting contour.**
The formulae to determine maximum deflections, maximum normal stresses in load-bearing layers for symmetric sandwich plates with same thickness isotropic outer layers are given in 8.2. Transverse deflection of sandwich plate is considered. The load shall be perpendicular to the plate plane.
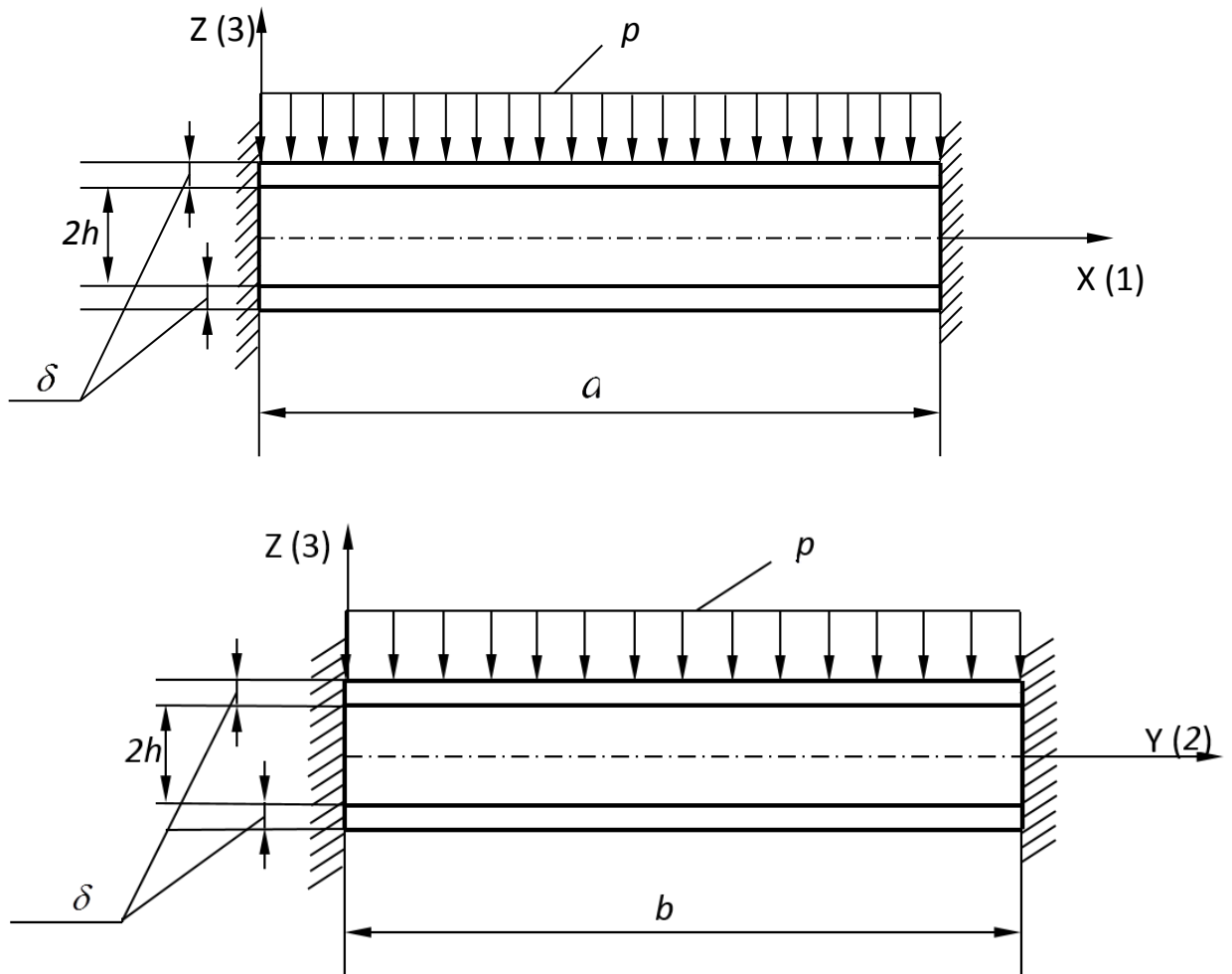

Fig. 8.3
Load type of the sandwich plate".

164   **New para 8.4** is introduced reading as follows:

"**8.4**   Plate deflection, in mm, is maximum at $x = a/2$, $y = b/2$ and determined by the formula

$$|w|_{x=a/2, \ y=b/2} = \frac{pb^2}{10^3(2h+\delta)}\left[\frac{m^1 b^2}{E_{bl}\delta(2h+\delta)} + \frac{\bar{m}_1}{G_{core}}\right],$$

where a = length of the sandwich plate, in m;

b = width of the sandwich plate, in m;
$2h$ = core thickness of the sandwich plate, in m;
δ = thickness of the load-bearing layer of the sandwich laminate, in m;
p = uniformly distributed load, in Pa;
E_{bl} = Young's modulus of load-bearing layers of the sandwich plate, in Pa;
G_{core} = shear modulus of the core in the sandwich plate, in Pa;
$\nu = \nu_{12(bl)}$ = Poisson's ratio of the material of load-bearing layers in the sandwich plate;
$m_1, \bar{m}_1$ = factors.

Values of factor m_1 depending on Poisson's ratio ν of the load-bearing layers of the sandwich plate and ratio of plate sides $\gamma = a/b$ are specified in Fig. 8.4-1.

Values of factor $\bar{m}_1$ depending on ratio of plate sides $\gamma = a/b$ are specified in Fig. 8.4-2.

Normal stresses σ_x, in Pa, are maximum at $x = 0; a, y = b/2$ and determined by the formula

$$|\sigma_x|_{x=0;\ a,y=b/2} = p\frac{b^2}{\delta^2}\frac{1+h/\delta}{(1+2h/\delta)^2}m_2,$$
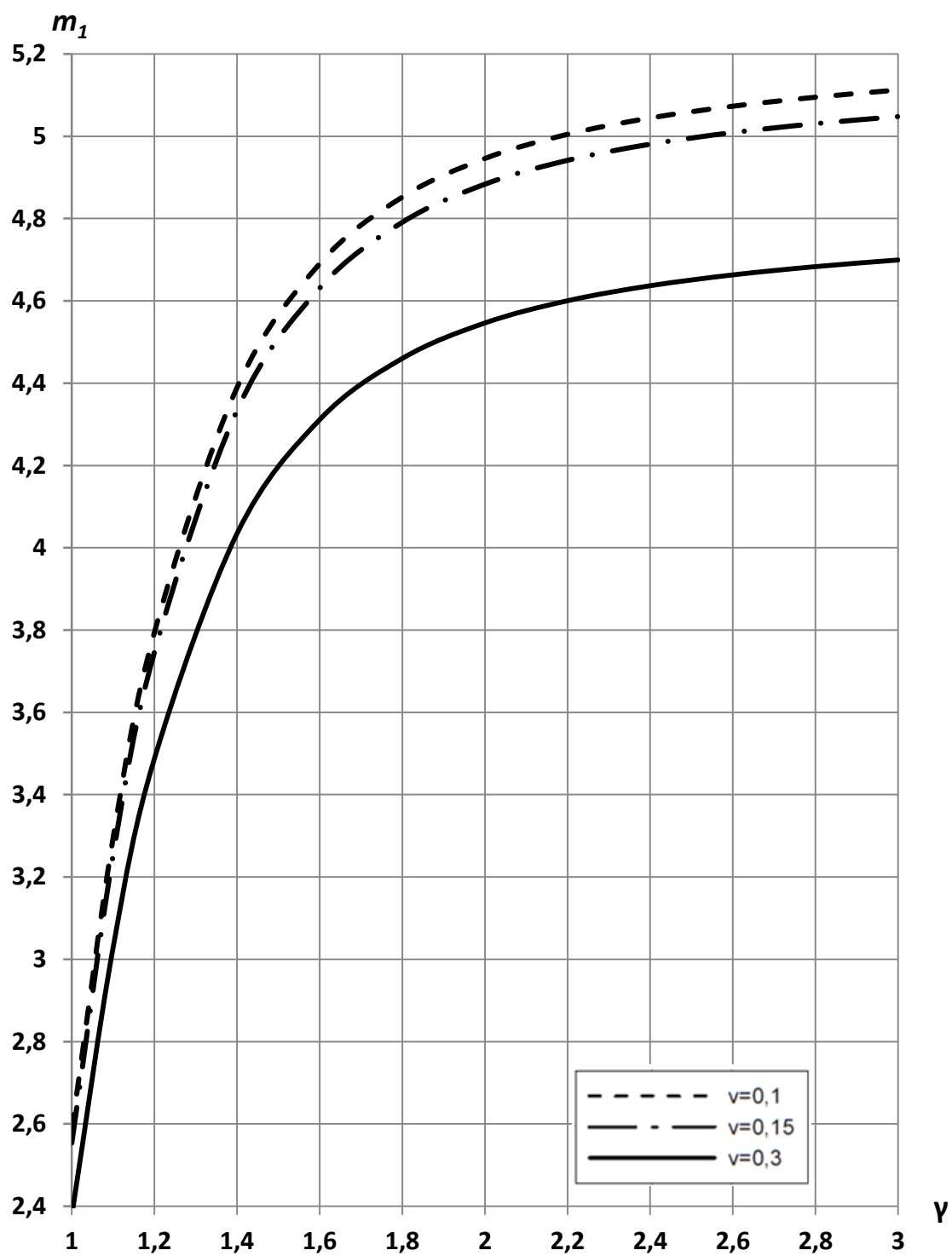
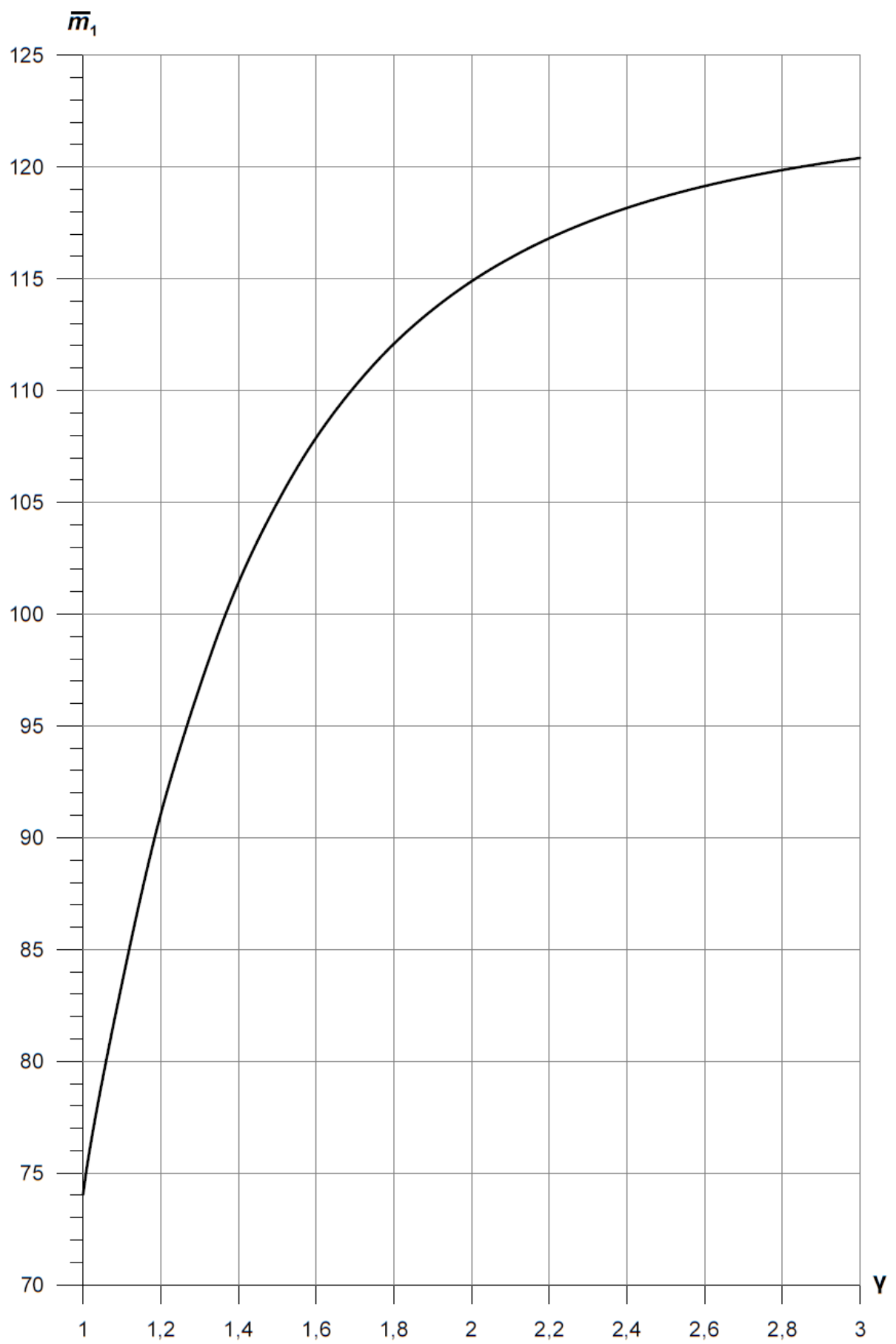where m_2 = factor.

Fig. 8.4-1
Values of factor m_1

Fig. 8.4-2
Values of factor $\bar{m}_1$

Normal stresses σ_y, in Pa, are maximum at $x = a/2, y = 0; b$ and determined by the formula

$$\left|\sigma_y\right|_{x=a/2,y=0;b} = p\,\frac{b^2}{\delta^2}\,\frac{1+h/\delta}{(1+2h/\delta)^2}\,m_3,$$

where m_3 = factor.

Values of factors m_2 and m_3 depending on Poisson's ratio ν of the load-bearing layers of the sandwich plate and ratio of plate sides $\gamma = a/b$ are specified in Figs. 8.4-3 — 8.4-4 accordingly.
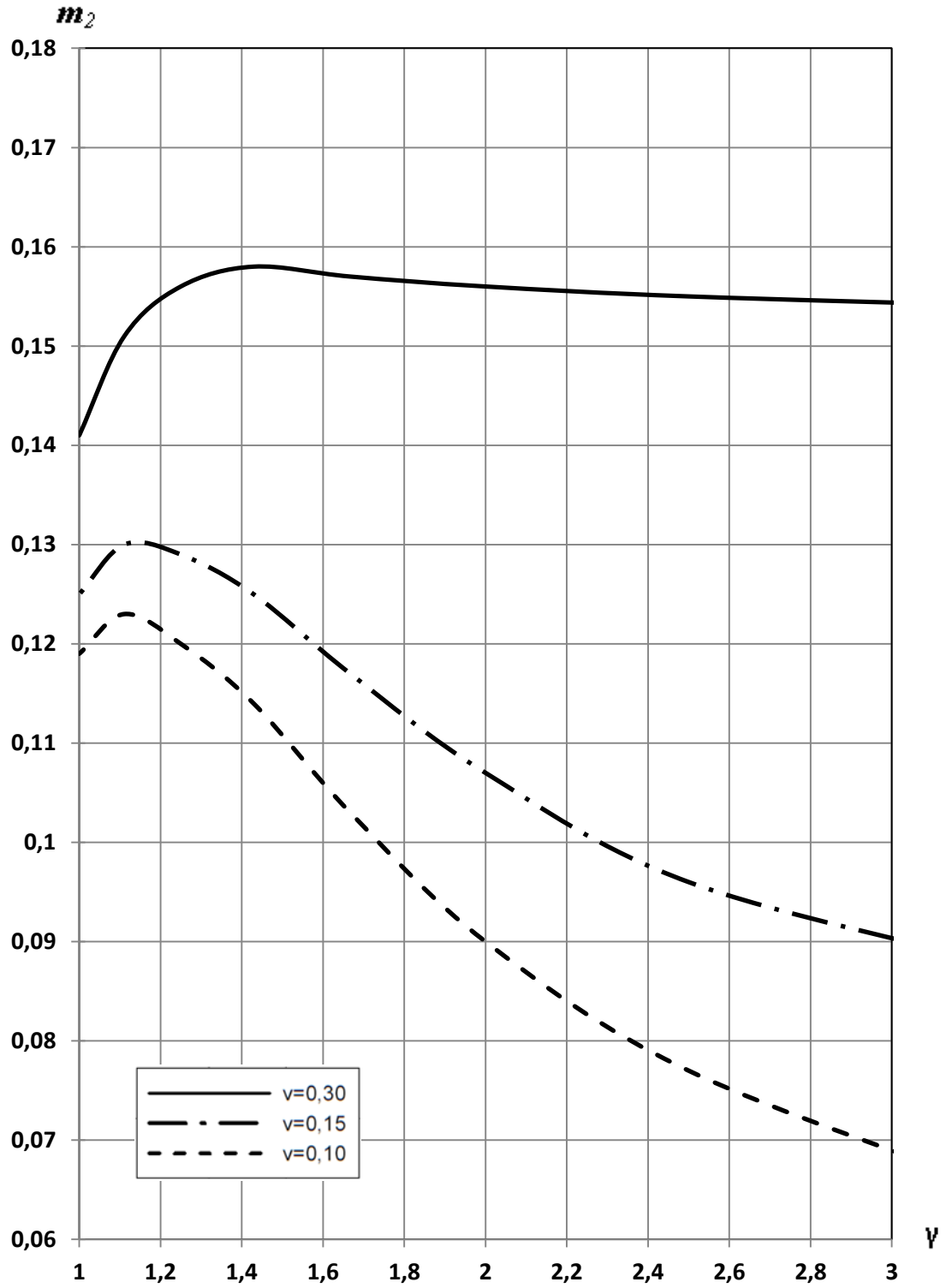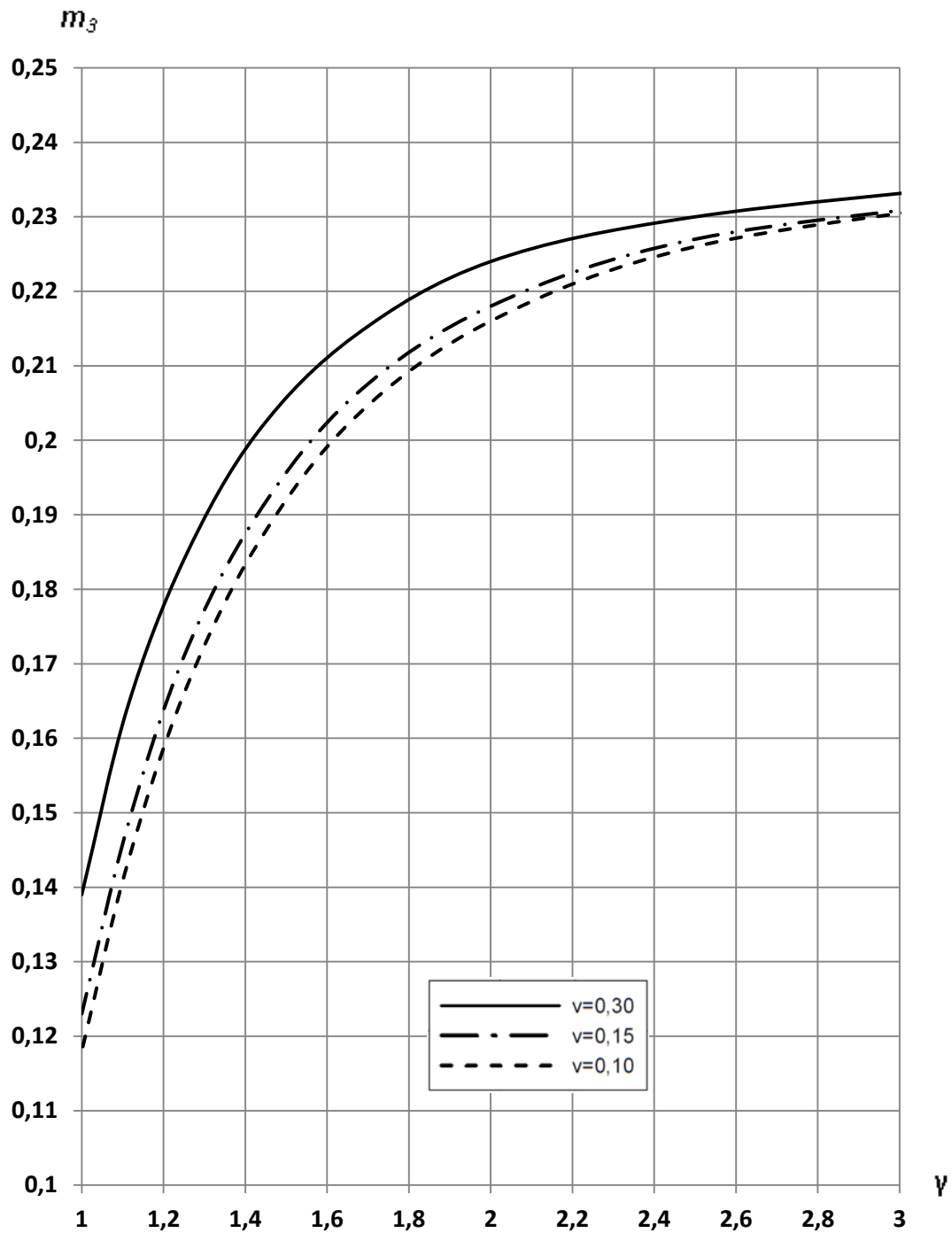

Fig. 8.4-3
Values of factor m_2

Fig. 8.4-4
Values of factor m_3".

9 BUCKLING STRENGTH OF SANDWICH PLATES

165   Preamble of **Section 9** is replaced by the following text:

"**9.1**   This procedure is intended for buckling strength calculation of sandwich plates with isotropic core. The procedure allows determining the critical buckling load at one-sided uniform compression, with edges attached in different ways.
    The calculation procedure is applied to rectangular symmetric plates over thickness $\delta_1 = \delta_2 = \delta$. Load-bearing layers and core are isotropic materials, i.e. for load-bearing layers and the core the following conditions are met accordingly:

$E_{i(bl1)} = E_{i(bl2)} = E_{bl}$; $v_{ij(bl1)} = v_{ij(bl2)} = v_{12(bl)}$;
$E_{i(core)} = E_{core}$; $G_{ij(core)} = G_{core}$; $v_{ij(core)} = v_{core}$.

This procedure may be also used for calculation of stress-strain behavior of sandwich plates with orthotropic load-bearing layers when $E_{1(bl)} > E_{2(bl)}$ and $(1 - E_{2(bl)}/E_{1(bl)}) \cdot 100\,\% < 20\,\%$, whereas the following conditions for geometric properties and elastic characteristics are met:

$$0,01 \leq \frac{G_{core}}{E_{1(bl)}} \leq 0,1; \ 0,01 \leq \frac{\delta}{h} \leq 0,25; \ \frac{2h}{a}\sqrt{1 + (a\,/\,b)^2} \leq 0,3.$$

In such case, the core takes up only transverse loads preventing contact between the layers.".

166   **Paras 9.1** and **9.2** are renumbered **9.2** and **9.3** accordingly.

167   **Figure 30** and references thereto are renumbered **9.2**.

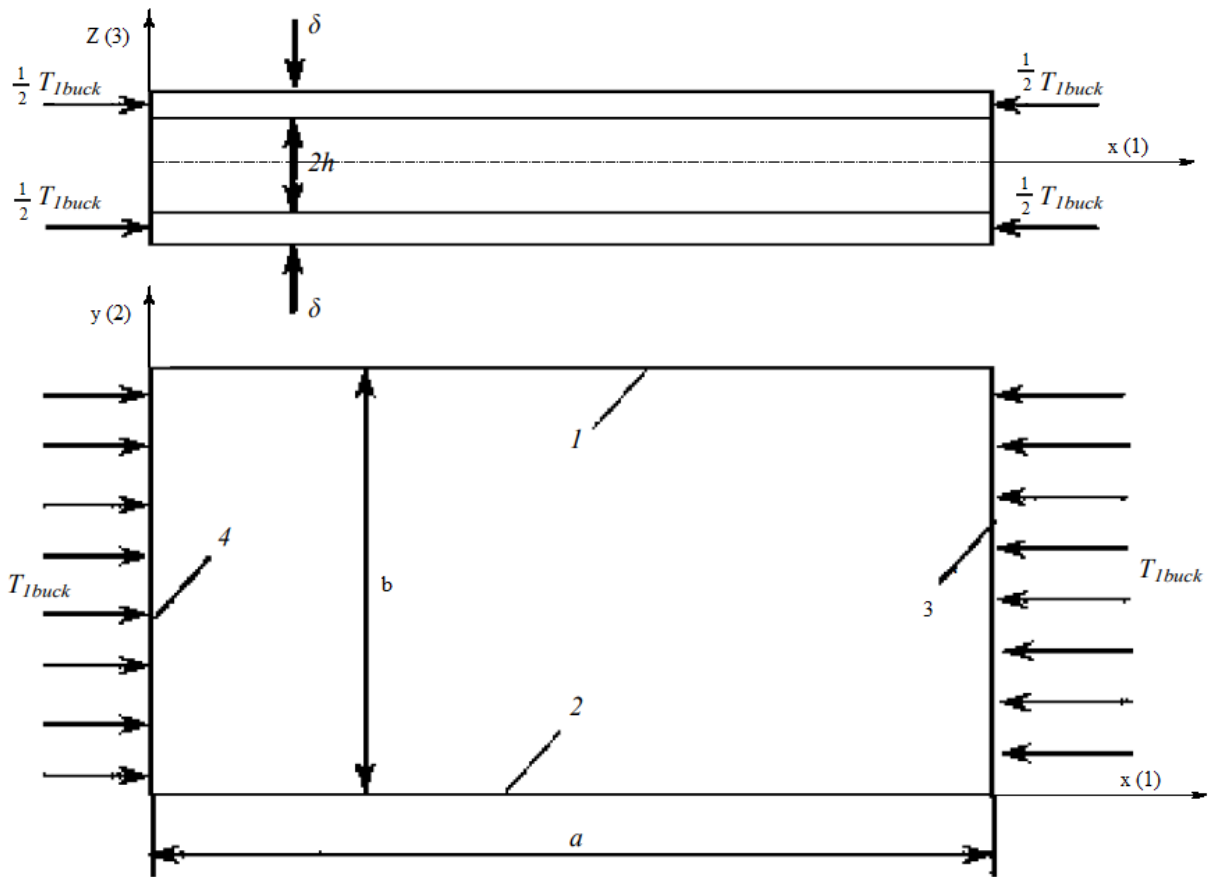168   **Figure 9.2** (former Figure 30) is replaced by the following one:

"

Fig. 9.2
Load type of a rectangular sandwich plate".

169   **Para 9.3** (former para 9.2) is replaced by the following text:

"**9.3**   Buckling load T_{1buck}, in N/m, is determined by the formula

$$T_{1buck} = m_t \frac{\pi^2 D}{b^2},$$

where $D = 2D_1 + D_{core} + 2B_1(h + \frac{\delta}{2})^2;$

$D_1 = \frac{E_{bl}\delta^3}{12(1-v_{12(bl)}^2)};$

$B_1 = \frac{E_{bl}\delta}{1-v_{12(bl)}^2};$

$D_{core} = \frac{2E_{core}h^3}{3(1-v_{core}^2)};$

E_{bl} = Young's modulus of load-bearing layers along the sandwich plate longer side, in Pa;

E_{core} = Young's modulus of the sandwich plate core, in Pa;

$v_{12(bl)}$ = Poisson's ratio of the material of load-bearing layers plane in the sandwich plate;

v_{core} = Poisson's ratio of the material of the sandwich plate core.

Where $\dfrac{h}{\delta} = 5$, buckling load T_{1buck}, in N/m, is determined by the formula

$$T_{1buck} = m_t m_m \frac{\pi^2 E_{core}\delta^3}{b^2},$$

where $m_m = \frac{2}{3}\left[\frac{91\eta}{1-v_{12(bl)}^2} + \frac{125}{(1-v_{core}^2)}\right], \eta = \frac{E_{bl}}{E_{core}}.$

Values of factor m_m with $v_{12(bl)} = 0,1÷0,2$ and $v_{core} = 0,3÷0,4$ are determined according to the diagrams provided in Fig. 9.3-1.

Values of factor m_t are determined according to the diagrams depending on the way in which the plate is supported (refer to Figs. 9.3-2 — 9.3-5), while stiffness characteristics are determined by the formulae specified in this Section.

Value of factor k for Figs. 9.3-2 — 9.3-5 is determined by the formula

$$k = \frac{\pi^2 B_0 h}{G_{core}b^2},$$

where $B_0 = 2B_1 + \frac{B_{core}}{3};$

$B_{core} = \frac{2E_{core}h}{1-v_{core}^2};$

G_{core} = shear modulus of the core in the sandwich plate, in Pa.".

170   **Figure 31** and references thereto are renumbered **9.3-1**.

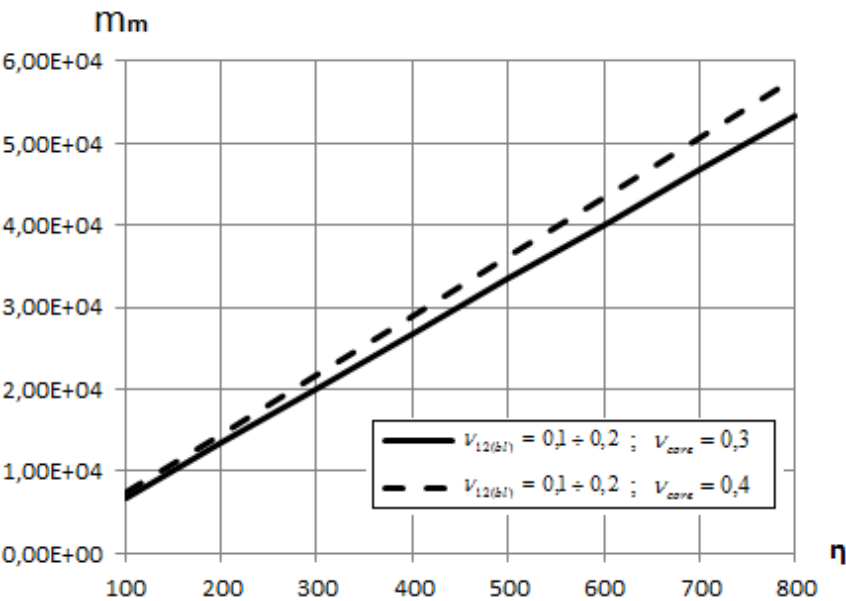171 **Figure 9.3-1** (former Figure 31) is replaced by the following one:

"

Fig. 9.3-1
Dependency diagram of factor m_m on ratio of moduli η ($v_{12(bl)} = 0{,}1\div0{,}2$ and $v_{core} = 0{,}3\div0{,}4$)".

172 **Figures 32 — 35** and references thereto are renumbered **9.3-2 — 9.3-5** accordingly.